We are IntechOpen,
the world's leading publisher of
Open Access books
Built by scientists, for scientists

7,200
Open access books available

190,000
International authors and editors

205M
Downloads

Our authors are among the

154
Countries delivered to

TOP 1%
most cited scientists

12.2%
Contributors from top 500 universities

CLARIVATE ANALYTICS
BOOK
CITATION
INDEX
INDEXED

WEB OF SCIENCE™

Selection of our books indexed in the Book Citation Index
in Web of Science™ Core Collection (BKCI)

Interested in publishing with us?
Contact book.department@intechopen.com

Model Predictive Control for Block-oriented Nonlinear Systems with Input Constraints

Hai-Tao Zhang[*]
Department of Control Science and Engineering
State Key Laboratory of Digital Manufacturing Equipment and Technology
Huazhong University of Science and Technology, Wuhan
P.R.China

1. Introduction

In process industry, there exist many systems which can be approximated by block-oriented nonlinear models, including Hammerstein and Wiener models. Hammerstein model consists of the cascade connection of a static (memoryless) nonlinear block followed by a dynamic linear block while Wiener model the reverse. Moreover, these systems are usually subjected to input constraints, which makes the control of block-oriented nonlinearities challenging.

In this chapter, a Multi-Channel Identification Algorithm (*MCIA*) for Hammerstein systems is first proposed, in which the coefficient parameters are identified by least squares estimation (*LSE*) together with singular value decomposition (*SVD*) technique. Compared with traditional single-channel identification algorithms, the present method can enhance the approximation accuracy remarkably, and provide consistent estimates even in the presence of colored output noises under relatively weak assumptions on the persistent excitation (PE) condition of the inputs.

Then, to facilitate the following controller design, the aforementioned *MCIA* is converted into a Two Stage Single-Channel Identification Algorithm (*TS-SCIA*), which preserves most of the advantages of *MCIA*. With this *TS-SCIA* as the inner model, a dual-mode Nonlinear Model Predictive Control (NMPC) algorithm is developed. In detail, over a finite horizon, an optimal input profile found by solving a open-loop optimal control problem drives the nonlinear system state into the terminal invariant set, afterwards a linear output-feedback controller steer the state to the origin asymptotically. In contrast to the traditional algorithms, the present method has a maximal stable region, a better steady-state performance and a lower computational complexity. Finally, a case study on a heat exchanger is presented to show the efficiency of both the identification and the control algorithms.

On the other hand, for Wiener systems with input constraints, since most of the existing control algorithms cannot guarantee to have sufficiently large regions of asymptotic stability, we adopted a subspace method to separate the nonlinear and linear blocks in a constrained multi-input/multi-output (MIMO) Wiener system and then developed a novel dual-mode

nonlinear model predictive control algorithm to maximize the region of the asymptotic stability. Simulation results are presented to demonstrate the superiority of this new control algorithm.

In sum, this chapter developed some new NMPC methods for block-oriented nonlinearities with input constraints. Meanwhile, these approaches can effectively enlarge the closed-loop stable area so as to extend the feasible working region and improve the reliability of the control systems in real process industrial applications.

2. Model Predictive Control for Hammerstein systems with input constraints

2.1 Introduction

In industrial processes (1), most dynamical systems can be better represented by nonlinear models, which are able to describe the systems over large operation ranges, rather than by linear ones that are only able to approximate the systems around given operation points (23; 48). One of the most frequently studied classes of nonlinear models is the Hammerstein model (17; 48), which consists of the cascade connection of a static (memoryless) nonlinear block followed by a dynamic linear block. Under certain considerations such as fading memory assumption (10) the Hammerstein approximation could be a good representation. Thus, this model structure has been successfully applied to chemical processes (heat exchanger (17), distillation (5; 17; 35)), biological processes (20; 30) signal processing (3; 55), and communications (3; 25)). In recent years, identification and control of Hammerstein systems has become one of the most needed and yet very difficult tasks in the field of the process industry.

In MPC (Model Predictive Control) framework (20; 32), the input is calculated by on-line minimization of a performance index based on model predictions. It is well known that the control quality relies on the accuracy of the model. In recent years, extensive efforts were devoted to modelling of Hammerstein nonlinearities (2; 17; 23; 26; 27; 31). For example, Bai (2) studied SISO (Single Input/ Single Output) systems subject to external white noise. Gómez and Baeyens (23) designed a non-iterative identification with guaranteed consistent estimation even in the present of coloured output noise. Both of their works use only one channel to identify the system, therefore, owing to the SVD (singular value decomposition) nature of their methods, the identification errors usually can not be minimized. A basic reason is that the error is determined by the second largest singular value (for SISO system) or the st largest singular value (for MIMO system with inputs) of the estimated coefficients matrix. For a SISO system, if the sampling set is not big enough or the PE (persistent excitation) conditions are not fulfilled, the second largest singular value can not be neglected, making the identification accuracy unsatisfactory or even unacceptable. On the other hand, the research on the control of Hammerstein systems is still on the midway so far. Most of the existent control algorithms have some of the following disadvantages

- Reliance on prior knowledge;

- Insufficiently large closed-loop stable regions;

- Limited capacity of handling input constraints.

In detail, Haddad and Chellaboina (28) suggested a design that can guarantee global asymptotic closed-loop stability for nonlinear passive systems by embedding a nonlinear dynamic compensator with a suitable input nonlinearity, which requires the memoryless

nonlinear block to be partially known or measurable without considering input constraints. Patwardhan *et al.* (51) used a PLS (Partial Least Square) framework to decompose the modelling problem into a series of univariate problems in the latent subspace while preserving optimality of the input constraints. In this way, they can extend the SISO formulation into a constrained MIMO scenario. In this approach, however, the computational complexity is prohibitive, and the reliance on prior knowledge can not be eliminated. Knohl *et al.* (40) slightly alleviated this reliance by an ANN (Artificial Neural Network) inverse compensation, which makes the control scheme more flexible, but its stable region is still small. Fruzzetti *et al.* (18) and *Zhu et al.* (71) developed GPC (Generalized Predictive Control) and MPC algorithms respectively by taking input constraints into account. These schemes still can not ensure a large stable region in general, and require prior knowledge of the real plant such as order, structure, partial coefficients, etc. Bolemen *et al.* (9) extended their own work (8) which preserves the convex property of the optimization problem, but does not consider input constraints. In order to enlarge the asymptotically stable region for constrained nonlinear systems, Chen and Allgöwer (14) developed a quasi-infinite horizon Nonlinear Model Predictive Control (NMPC) algorithms based on a dual-mode (or two-step) technique, which has opened a new avenue in this fascinating field. Among the various following works of Chen and Allgöwer's work (14), there are three important investigations made by Kouvartakis *et al.* (41) Lin *et al.* (44) and Ding *et al.* (16). More precisely, Kouvartakis *et al.* (41) proposed a new approach that deployed a fixed state-feedback law with the assistance of extra degrees of freedom through the use of perturbations, which led to a significant reduction in computational cost. More generally, for linear systems with actuator rate constraint, Lin *et al.* (44) designed both state-feedback and output-feedback control laws that achieve semi-global asymptotic stabilization based on the assumption of detectability of the system. For input saturated Hammerstein systems, Ding *et al.* (16) designed a two-step MPC by solving nonlinear algebraic equation group and deconstraint. The stable region is enlarged and its domain of attraction is designed applying semi-global stabilization techniques. Unfortunately, this nice work is still based on the measurability of the state of the linear block.

Based on the above analysis, two important tasks are formulated as follows:

- *Task one*: Develop a better identification algorithm to separate the nonlinear/linear blocks of the Hammerstein system more effectively so that some mature linear control theories can be used to facilitate the nonlinear control algorithm design.

- *Task two*: Develop a more efficient control algorithm for constrained Hammerstein systems.

Bearing these tasks in mind, we propose a NMPC algorithm based on a Two Stage Single-Channel Identification Algorithm (TS-SCIA) (68). More precisely:

- A Multi-Channel Identification Algorithm (MCIA) is developed for Hammerstein systems which eliminates requirement of prior knowledge about the plant and minimizes the identification errors. The MCIA is then converted to a TS-SCIA thereby facilitating the controller design. A sufficient condition for the convergence and approximation capability is given for the new algorithm.

- A dual-mode NMPC algorithm is developed by taking the above mentioned Two Stage Single-Channel Identification Model (TS-SCIM) as the internal model. The closed-loop stable region is maximized by using ellipsoidal invariant set theory together with linear matrix inequality (LMI) techniques.

2.2 Model identification

The key problem on this issue is how to efficiently separate the coefficients of the linear and nonlinear blocks, namely nonlinear/linear separation. A number of approaches are previously proposed: these include the singular value decomposition (SVD) combined with least square estimation (LSE) (23), iterative finite response (FIR) method (45), separable LSE (63), Hunter-Korenberg iteration (35) , correlation analysis (4) and so on. Among them, SVD-LSE approach is one of the most extensively studied and most widely applied methods. In this approach, the system output $y(t)$ is expanded as

$$\begin{aligned} y(t) &= G(z^{-1})\mathcal{N}(u(t)) + \xi(t) \\ &= \sum_{k=1}^{N} c_k x_k(z^{-1}) \sum_{i=1}^{r} a_i g_i(u(t)) + \xi(t), \end{aligned} \tag{1}$$

where $u(t) \in \mathbb{D} \subset \mathbb{R}^n$, $v(t) = \mathcal{N}(u(t)) \in \mathbb{R}^n$, $y(t) \in \mathbb{R}^m$ and $\xi(t) \in \mathbb{R}^m$ are the input, intermediate variable, output and external noise vector at time t, respectively. External noise $\xi(t)$ can be white or colored noise sequence induced by measurement or external disturbances, and input signal $u(t)$ can be random or stationary. $G(z^{-1})$ and $\mathcal{N}(\cdot)$ denote the linear and nonlinear blocks expanded by suitable orthonormal and nonlinear bases $x_k(z^{-1})$ and $g_i(\cdot)$, respectively. The sequences $\left\{c_k \in \mathbb{R}^{m \times n}\right\}_{k=1}^{N}$ and $\left\{a_i \in \mathbb{R}^{n \times n}\right\}_{i=1}^{r}$ are the coefficients of the linear and nonlinear blocks, respectively, and z^{-1} is the one-step backward shifting operator, i.e. $z^{-1}u(t) = u(t-1)$. The state $x_k(z^{-1})$ could be Jacobi series [13], spline functional series (**?**), orthonormal functional series (OFS, including Laguerre series (19; 60; 66; 67; 69), Kautz series (19; 33) and so on) or some others.

Actually, in recent years, extensive efforts (23) were devoted to this kind of SVD-LSE approaches. For example, Bai (2) studied SISO (Single Input/ Single Output) systems subject to external white noise. Gómez and Baeyens (23) designed a non-iterative identification with guaranteed consistent estimation even in the present of colored output noise. Both of their works use merely one channel to identify the system, therefore, owing to the SVD nature of their methods, the identification errors usually can not be minimized. A basic reason is that, for the Hammerstein system (1), the error is determined by the $(n+1)$th largest singular value the estimated coefficients matrix. If the sampling set is not big enough or the PE (persistent excitation) conditions are not fulfilled, the $(n+1)$th largest singular value can not be neglected, making the identification accuracy unsatisfactory or unacceptable, especially for small numbers of truncation lengths of the nonlinear/linear basis series, i.e. r and N (see Eq. (1)). In brief, it is an urgent task to develop a better identification algorithm to separate the nonlinear/linear blocks of the Hammerstein system more effectively.

In this section, we argue that the single-channel separation is a bottleneck to better modeling accuracy, and adding more identification channels can effectively enhance the performance, for they have the capability to compensate the residuals of the single-channel nonlinear/linear separation.

Fig. 1(a) shows the implementary details on a single identification channel of the present modeling method. First, system input $u(t)$ is fed into parallel weighted nonlinear bases to produce the intermediate variable $v(t)$. According to *Weierstrass Theorem* (42) (every continuous function defined on a finite region can be uniformly approximated as closely as desired by a polynomial function), the bases are generally chosen as polynomial bases. Then $v(t)$ is injected into the linear OFS filter, through which the filter output sequence can be yielded.
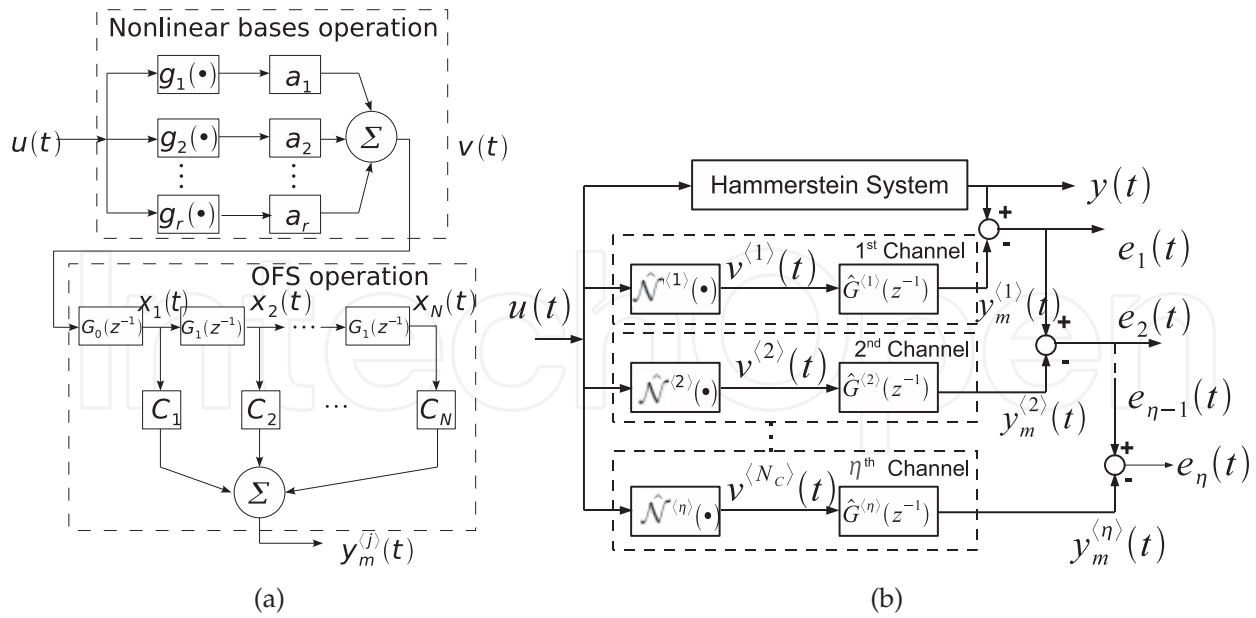
Fig. 1. (Color online) (a): Implementary details of each modeling channel; (b): Multi-channel identification

Since $\{x_k(t)\}_{k=1}^{\infty}$ forms a complete orthonormal set in functional space $\mathcal{L}_2(\mathbb{R}^+)$ (33; 66–68), each stable linear system can be approximately represented as $h(t) = \sum_{k=1}^{N} c_k \varphi_k(t)$, where $\{c_k\}_{k=1}^{N}$ are the coefficients of the linear block, the Laguerre function $\varphi_k(t)$ is given in (33; 66), and the kth order filter output is calculated by $x_k(t) = \int_0^{\infty} \varphi_k(\tau) v(t - \tau) d\tau$. To get the OFS filter output sequence, one should pre-calculate all the OFS according to the state equation $x(t + 1) = Ax(t) + Bv(t)$, where A and B are pre-optimized matrices (33; 66). As shown in Fig. 1, the first-order filters is the Laguerre series, in which

$$
\begin{aligned}
G_0(z^{-1}) &= z^{-1}\sqrt{1 - p^2}/(1 - z^{-1}p), \\
G_1(z^{-1}) &= (z^{-1} - p)/(1 - z^{-1}p),
\end{aligned}
\tag{2}
$$

where p is the filter pole. The second-order OFS is the Kautz Series, in which $G_0(z^{-1})$ and $G_1(z^{-1})$ are the second order OFS transfer functions. Analogically, Heuberger *et al.* (33) introduced the higher-order OFS models. As the order increases, OFS model can handle more complex dynamics. Finally, the model is obtained by synthesizing the OFS filter output sequence and their corresponding coefficients according to $y_m(t) = \sum_{k=1}^{N} c_k x_k(t)$ which leads to Eq. (2). Consequently, considering the S-point data set suffered by external noise sequence $\{\xi(t)\}_{t=1,\cdots,S}$, Eq. (1) can be rewritten in a linear regressor form as

$$
Y_S = \Phi_S^T \theta + \Upsilon_S,
\tag{3}
$$

with

$$
\begin{aligned}
Y_S &\triangleq [y(1), \cdots, y(S)]^T, \\
\Upsilon_S &\triangleq [\xi(1), \cdots, \xi(S)]^T, \\
\theta &\triangleq [c_1 a_1, \cdots, c_1 a_r, \cdots, c_N a_1, \cdots, c_N a_r]^T, \\
\Phi_S &\triangleq [\phi(1), \cdots, \phi(S)]^T,
\end{aligned}
$$

and

$$\phi(t) \triangleq \left[x_1(z^{-1})g_1^T(u(t)), \cdots, x_1(z^{-1})g_r^T(u(t)), \cdots, \right.$$
$$\left. x_N(z^{-1})g_1^T(u(t)), \cdots, x_N(z^{-1})g_r^T(u(t)) \right]^T, \quad (4)$$

where the superscript 'T' means transpose. Note that in real applications, the orthonormal basis $x_k(z^{-1})g_i^T(u(t))$ ($k = 1, \cdots, N$; $i = 1, \cdots, r$) and the system output $y(t)$ in Eq. (1) are calculated according to the state-space equations in (62; 66; 67). As shown in Fig. 1(a), kernel matrix Φ_S is obtained by carrying out nonlinear bases and OFS operations on the input sequence, and θ is the coefficient vector of Φ_S. Then, provided the indicated inverse exists, it is well known that the LSE $\hat{\theta}$ of minimizing the prediction errors $\varepsilon_s = Y_S - \Phi_S^T \theta$ is calculated by (46)

$$\hat{\theta} \triangleq (\Phi_S \Phi_S^T)^{-1} \Phi_S Y_S. \quad (5)$$

Define $\Theta_{ac} \triangleq \left\{ a_i^T c_j^T \right\}_{1 \leq i \leq r; 1 \leq j \leq N} = ac^T$ with $a \triangleq [a_1, \cdots, a_r]^T$ and $c \triangleq [c_1^T, \cdots, c_N^T]^T$, it can be seen that θ is the block column matrix obtained by stacking the block columns of Θ_{ac} on the top one by one. Now, the problem is how to separate the nonlinear/linear coefficient parameter matrices a and c from the LSE $\hat{\Theta}_{ac}$ of Θ_{ac}. It is clear that feasible estimates $\hat{a}$ and $\hat{c}$ are the solutions of the optimization problem

$$(\hat{a}, \hat{c}) = \arg \min_{a,c} \left\| \hat{\Theta}_{ac} - ac^T \right\|_2^2. \quad (6)$$

This problem can be solved by the standard SVD (22) with the prerequisite $\|a_i\|_2 = 1$ ($i = 1, \cdots, r$). However, bearing the spectral nature of SVD in mind, one can easily find that the closest estimates of $\{a, c\}$ are not a single pair $\{\hat{a}, \hat{c}\}$ but a series of pairs $\left\{ \hat{a}^{\langle j \rangle}, \hat{c}^{\langle j \rangle} \right\}_{j=1}^{\eta}$, which solves the optimization problem

$$(\hat{a}^{\langle j \rangle}, \hat{c}^{\langle j \rangle})_{j=1}^{\eta} = \arg \min_{a^{\langle j \rangle}, c^{\langle j \rangle}} \left\| \hat{\Theta}_{ac} - \sum_{j=1}^{\eta} a^{\langle j \rangle} (c^{\langle j \rangle})^T \right\|_2^2. \quad (7)$$

From now on, the pair $\left\{ \hat{a}^{\langle j \rangle}, \hat{c}^{\langle j \rangle} \right\}$ is defined as the jth **identification channel**, with j and η denoting the sequence index and number of the identification channels, respectively. Therefore, in order to separate the nonlinear/linear blocks more effectively, more channels should be used to compensate the separation residuals of the single-channel method (23). To explain it more clearly, we will give a lemma and a theorem as follows. Note that, for the Hammerstein system (1), the multi-channel estimates $\hat{a}^{\langle j \rangle} \in \mathbb{R}^{rn \times n}$ and $\hat{c}^{\langle j \rangle} \in \mathbb{R}^{Nm \times n}$. In special, for SISO case, i.e. $m = 1$ and $n = 1$, the estimates $\hat{a}^{\langle j \rangle}$ and $\hat{c}^{\langle j \rangle}$ are all column vectors.

Lemma 1. *Let $rank(\Theta_{ac}) = \gamma$, here $\hat{\Theta}_{ac}$ is the estimate of Θ_{ac}, then the SVD of Θ_{ac} is*

$$\hat{\Theta}_{ac} = U_\gamma \Sigma_\gamma V_\gamma^T = \sum_{j=1}^{\gamma} \sigma_j \mu_j v_j^T \quad (8)$$

such that the singular value matrix $\Sigma_\gamma = diag \left\{ \sigma_j \right\}$ ($j = 1, \cdots, \min(r, N)$) satisfies $\sigma_1 \geq \cdots \geq \sigma_\gamma > 0$ and $\sigma_l = 0$ ($l > \gamma$), where μ_j and v_j ($j = 1, \cdots, \gamma$) are pairwise orthogonal vectors. If $\|a^{\langle j \rangle}\|_2 = 1$, then $\forall \eta$ ($1 \leq \eta \leq \gamma$), each identification channel can be calculated as below according to the optimization problem (7)

$$(\hat{a}^{\langle j\rangle}, \hat{c}^{\langle j\rangle}) = (\mu_j, \sigma_j v_j) \ (j = 1, \cdots, \eta) \tag{9}$$

with approximation error e_η given by

$$e_\eta = \left\| \hat{\Theta}_{ac} - \sum_{j=1}^{\eta} a^{\langle j\rangle}(c^{\langle j\rangle})^T \right\|_2^2 = \sum_{j=\eta+1}^{\gamma} \sigma_j^2. \tag{10}$$

It can be seen from Lemma 1 that after the SVD operation, $\hat{\Theta}_{ac}$ is decomposed into a series of pairs (or channels) $(\hat{a}^{\langle j\rangle}, \hat{c}^{\langle j\rangle})$. More precisely, as shown in Fig. 1(b), first the 1st channel model is estimated using the basic identification algorithm (30) from input-output data $\{u(t), y(t)\}_{t=1}^{S}$. Afterwards, the 1st channel model error $e_1(t) = y(t) - y_m^{\langle 1\rangle}$ is used to identify the 2nd channel model. Analogously, $e_2(t), \cdots, e_{\eta-1}(t)$ determine the 3rd, $\cdots$, ηth channel models, respectively. The approximation accuracy enhancement will be proven by the following theorem.

Theorem 1. *For the Hammerstein system (1), with the identification matrix calculated by Eq. (22), if $\mathrm{rank}(\hat{\Theta}_{ac}) = \gamma$, then, with the identification pairs $(\hat{a}^{\langle j\rangle}, \hat{c}^{\langle j\rangle})$ obtained by Eqs. (8) and (9) and the identification error index defined by Eq. (10), one has*

$$e_1 > e_2 > \cdots > e_\gamma = 0.$$

In other words, the the identification error decreases along with the increasing η.

Proof: This can be easily drawn from Lemma 1. ∎

In principle, one can select a suitable η according to the approximation error tolerance $\bar{e}$ and Eq. (10). Even for the extreme case that $\bar{e} = 0$, one can still set $\eta = \gamma$ to eliminate the approximation error, thus such suitable η is always feasible. For simplicity, if $\gamma \geq 3$, the general parameter setting $\eta = 2$ or 3 works well enough.

According to the conclusions of Lemma 1 and Theorem 1, multi-channel model $y_m(t) = \sum_{j=1}^{\eta} \hat{G}^{\langle j\rangle}(z^{-1})\hat{\mathcal{N}}^{\langle j\rangle}(u(t))$ outperforms single-channel model $y_m(t) = \hat{G}(z^{-1})\hat{\mathcal{N}}(u(t))$ in modeling accuracy. We hereby design a Multi-Channel Identification Algorithm (MCIA) based on Theorem 1 as follows. As shown in Fig. 1(b), the Multi-Channel Identification Model (MCIM) is composed of η parallel channels, each of which consists of a static nonlinear block described by a series of nonlinear basis $\{g_1(\cdot), \cdots, g_r(\cdot)\}$, followed by a dynamic linear block represented by the discrete Laguerre model (33; 60; 67; 69) in the state-space form (62; 66; 67). Without loss of generality, the nonlinears bases are chosen as polynomial function bases. Thus, each channel of the MCIM, as shown in Fig. 1, is described by

$$x^{\langle j\rangle}(t+1) = A x^{\langle j\rangle}(t) + B \sum_{i=1}^{r} \hat{a}_i^{\langle j\rangle} g_i(u(t)) \tag{11}$$

$$y_m^{\langle j\rangle} = (\hat{c}^{\langle j\rangle})^T x^{\langle j\rangle}(t) \ (j = 1, \cdots, \eta), \tag{12}$$

where $y_m^{\langle j\rangle}(t)$ and $x^{\langle j\rangle}(t)$ denote the output and state vector of the jth channel, respectively. Finally, the output of the MCIM can be synthesized by

$$y_m(t) = \sum_{j=1}^{\eta} y_m^{\langle j\rangle}(t) \tag{13}$$

Next, we will give a convergence theorem to support the MCIA.

Theorem 2. *For a Hammerstein system (1) with $\|a_i\|_2 = 1$ $(i = 1, \cdots, r)$, nominal output $\bar{y}(t) = \sum_{k=1}^{N} c_k x_k(z^{-1}) \sum_{i=1}^{r} a_i g_i(u(t))$ and allowable input signal set $\mathbb{D} \subset \mathbb{R}^n$. If the regressor $\phi(t)$ given by Eq. (4) is PE in the sense that for an arbitrary positive integer t_0 there exist some integer N_1 and positive constants α_1 and α_2 such that*

$$0 < \alpha_1 I \leq \sum_{t=t_0}^{t_0+N_1} \phi^T(t)\phi(t) \leq \alpha_2, \tag{14}$$

then

$$\sum_{j=1}^{\eta} \hat{a}^{\langle j \rangle}(\hat{c}^{\langle j \rangle})^T \xrightarrow{\text{a.s.}} \Theta_{ac} \tag{15}$$

$$y_m \xrightarrow{\text{a.s.}} \bar{y}(t) \tag{16}$$

where the symbol '$\xrightarrow{\text{a.s.}}$' denotes 'converge with probability one as the number of the data points S tends to infinity', and the model output $y_m(t)$ is determined by Eqs. (11), (12) and (13).

Proof: Since the linear block is stable, and $g_i(u(t))$ $(i = 1, \cdots, r)$ is bounded (because $u(t) \in \mathbb{D}$ is bounded and $g(\cdot)$ are nonlinear basis functions), the model output $y_m(t)$ is also bounded. Taking Eqs. (3) and (11) into consideration, one has that $\|\phi(t)\|_2$ is bounded, i.e. $\exists \delta_L > 0$, such that $\|\phi(t)\|_2 \leq \delta_L$. On the other hand, $\forall \varepsilon > 0$, $\exists \varepsilon_1, \varepsilon_2 > 0$ such that $\varepsilon = \varepsilon_1 + \varepsilon_2$. Let $\varepsilon_3 = \varepsilon_1 / (\delta_L \max(r, N))$ and $\varepsilon_4 = \varepsilon_2 / \delta_L$. Since the regressor $\phi(t)$ is PE in the sense of Eq. (14), one has that the estimate θ is strongly consistent in the sense that $\theta \to \hat{\theta}$ with probability one as $S \to \infty$ (denoted $\hat{\theta} \xrightarrow{\text{a.s.}} \theta$) (46), in other words, $\forall \varepsilon_4 > 0$, $\exists N_0 > 1$ such that $\|\hat{\theta} - \theta\|_2^2 \leq \varepsilon_4$ with probability one for $S > N_0$. Moreover, the consistency of the estimate $\hat{\theta}$ holds even in the presence of colored noise ξ (23). The convergence of the estimate $\hat{\theta}$ implies that

$$\hat{\Theta}_{ac} \xrightarrow{\text{a.s.}} \Theta_{ac} \tag{17}$$

Note that the consistency of the estimation $\hat{\theta}$ holds even in the presence of colored output noise (23).
Using Lemma 1 and assuming $\text{rank}(\hat{\Theta}_{ac}) = \gamma$, one gets from Theorem 1 that $\forall \varepsilon_3 > 0$, $\exists \eta \leq \gamma$ such that $\sum_{\eta+1}^{\gamma} \sigma_j \mu_j \varphi v_j^T \leq \varepsilon_3$, in other words, $\left\| \sum_{j=1}^{\eta} \hat{a}^{\langle j \rangle}(\hat{c}^{\langle j \rangle})^T - \hat{\Theta}_{ac} \right\|_2^2 \leq \varepsilon_3$ or

$$\sum_{j=1}^{\eta} \hat{a}^{\langle j \rangle}(\hat{c}^{\langle j \rangle})^T \to \hat{\Theta}_{ac}. \tag{18}$$

Thereby, substituting Eq. (18) into Eq. (17) yields Eq. (15). Furthermore, define

$$\hat{\theta}^{\langle j \rangle} \triangleq [\hat{c}_1^{\langle j \rangle} \hat{a}_1^{\langle j \rangle}, \cdots, \hat{c}_1^{\langle j \rangle} \hat{a}_r^{\langle j \rangle}, \hat{c}_2^{\langle j \rangle} \hat{a}_1^{\langle j \rangle},$$

$$\cdots, \hat{c}_2^{\langle j \rangle} \hat{a}_r^{\langle j \rangle}, \cdots, \hat{c}_N^{\langle j \rangle} \hat{a}_1^{\langle j \rangle}, \cdots, \hat{c}_N^{\langle j \rangle} \hat{a}_r^{\langle j \rangle}]^T,$$

then $\forall S > N_0$, the following inequality holds with probability one

$$
\begin{aligned}
[y_m(t) - \bar{y}(t)]^2 &= \left[\phi^T(t)(\textstyle\sum_{j=1}^{\eta} \hat{\theta}^{\langle j \rangle} - \hat{\theta} + \hat{\theta} - \theta)\right]^2 \\
&\leq \delta_L \left\|\textstyle\sum_{j=1}^{\eta} \hat{\theta}^{\langle j \rangle} - \hat{\theta}\right\|_2^2 + \delta_L \left\|\bar{\theta} - \theta\right\|_2^2 \\
&\leq \delta_L \max(r, N) \left\|\textstyle\sum_{j=1}^{\eta} \sigma_j \mu_j \varphi \nu_j^T - \hat{\Theta}_{ac}\right\|_2^2 + \delta_L \left\|\bar{\theta} - \theta\right\|_2^2 \\
&= \delta_L \max(r, N)\varepsilon_3 + \delta_L \varepsilon_4 = \varepsilon,
\end{aligned}
$$

where the definition of matrix 2-norm is given in (23). Thus, the conclusion (16) holds. This completes the proof. ∎

Thus, it is drawn from Theorems 1 and 2 that the increase of the identification channel number will help decrease the identification errors, which is the main theoretical contribution of this section.

2.3 Controller design
A Hammerstein system consists of the cascade connection of a static (memoryless) nonlinear block $\mathcal{N}(\cdot)$ followed by a dynamic linear block with state-space expression (A, B, C) as below

$$
\begin{aligned}
\dot{x} &= Ax + Bv, y = Cx, \\
v &= \mathcal{N}(u),
\end{aligned}
\tag{19}
$$

with $u(t) \in [-\bar{u}, \bar{u}]$. Naturally, a standard output feedback control law can be derived by (13)

$$
\begin{aligned}
v &= K\hat{x} \\
u &= \mathcal{N}^{-1}(v),
\end{aligned}
\tag{20}
$$

where $\hat{x}$ is the estimation of x by some state observer L, $\mathcal{N}^{-1}(\cdot)$ is the inverse of $\mathcal{N}(\cdot)$, and the closed-loop state matrix $A + BK$ and observer matrix $A_L C$ are designed Hurwitz. Now, the *problem* addressed in this section becomes optimize such an output-feedback controller for the Hammerstein system (19) such that the closed-loop stability region is maximized and hence the settling time is substantially abbreviated.
The nonlinear block $\mathcal{N}(\cdot)$ can be described as (68):

$$
\mathcal{N}(z(t)) = \sum_{r=1}^{N} a_i g_i(z(t)),
\tag{21}
$$

where $g_i(\cdot) : \mathbb{R} \to \mathbb{R}$ are known nonlinear basis functions, and a_i are unknown matrix coefficient parameters. Here, $g_i(\cdot)$ can be chosen as polynomials, radial basis functions (RBF), wavelets, etc. At the modeling stage, the sequence $v(t_j)$ ($j = 1, \cdots, N$) is obtainable with a given input sequence $u(t_j)$ ($j = 1, \cdots, N$) and an arbitrary initial state $x(0)$. Thereby, according to Lease Square Estimation (LSE), the coefficient vector $a := [a_1, \cdots, a_N]^T$ can be identified by

$$
\hat{a} = (G^T G)^{-1} G^T v
\tag{22}
$$

with

$$
G = \begin{bmatrix} g_1(t_1) & \cdots & g_N(t_1) \\ & \vdots & \\ g_1(t_s) & \cdots & g_N(t_s) \end{bmatrix},
$$

$v = [v(t_1), \cdots, v(t_N)]^T$ and $s \geq N$. Note that $\hat{a}$ is the estimation of a, which is an consistent one even in the presence of colored external noise.

Now the intermediate variable control law $v(t)$ in Eq. (19) can be designed based on the linear block dynamics. Afterwards, one can calculate the control law $u(t)$ according to the inverse of $v(t)$. Hence, for the Hammerstein system (19), suppose the following two assumptions hold:

A1 The nonlinear coefficient vector a can be accurate identified by the LSE (22), i.e., $\hat{a} = a$;

A2 For $|u(t)| \leq \bar{u}$, the inverse of $\mathcal{N}(\cdot)$ exists such that

$$
\mathcal{N}(\mathcal{N}_Z^{-1}(v(t))) := \tilde{v}(t) = (1 + \delta(v(t)))v(t),
$$

where $\delta(v(t))) < \sigma$ ($\sigma \in \mathbb{R}^+$), and $\mathcal{N}_Z^{-1}$ denotes the inverse of $\mathcal{N}(\cdot)$ calculated by some suitable nonlinear inverse algorithm, such as Zorin method (21).

For conciseness, we denote $\delta(v(k))$ by $\delta(\cdot)$, and hence, after discretization, the controlled plant is described as follows:

$$
x(k+1) = Ax(k) + B\tilde{v}(k) = Ax(k) + B(1 + \delta(\cdot))v(k),
$$
$$
y(k) = Cx(k). \tag{23}
$$

Afterwards, a state observer $L \in R^N$ is used to estimate $x(k)$ as follows:

$$
\hat{x}(k+1) = A\hat{x}(k) + B(1 + \delta(\cdot))v(k) + LCe(k), \tag{24}
$$
$$
e(k+1) = \Phi e(k), \tag{25}
$$

where $\hat{x}$ is the estimation of x, $e(k) := x(k) - \hat{x}(k)$ is the state estimation error, and the matrix $\Phi = A - LC$ is designed as Hurwitz. Then, an NMPC law is designed with an additional term $D(k+i|k)$ as follows:

$$
v(k+i|k) = K\hat{x}(k+i|k) + ED(k+i|k),
$$
$$
u(k|k) = \mathcal{N}_z^{-1}((v(k|k))), \tag{26}
$$

where $E := [1, 0, \cdots, 0]_{1 \times M}$, $\hat{x}(k|k) := \hat{x}(k)$, $v(k|k) := v(k)$, and $D(k|k) := D(k) = [d(k), \cdots, d(k + M - 1)]^T$ is defined as a perturbation signal vector representing extra degree of freedom. Hence the role of $D(k)$ is merely to ensure the feasibility of the control law (26), and $D(k+i|k)$ is designed such that

$$
D(k+1|k) = TD(k+i-1|k) \ (i = 1, \cdots, M),
$$

where

$$
T = \begin{bmatrix} \mathbf{0} & I_{(M-1) \times (M-1)} \\ 0 & \mathbf{0}^T \end{bmatrix}_{M \times M},
$$

$M \geq 2$ is the prediction horizon and **0** is compatible zero column vector. Then, substituting Eq. (26) into Eq. (24) yields

$$\hat{z}(k+i|k)) = \Pi \hat{z}(x+k-i|k)$$
$$+[(\delta(\cdot)B\bar{K})^T, 0]^T \hat{z}(k+i-1/k)$$
$$+[(LC)^T, 0]^T e(k+i-1|k), \ (i=1,\cdots,M) \tag{27}$$

with $\hat{z}(k+i|k) = [\hat{x}^T(k+i|k), D(k+i|k)^T]^T$, $\Pi = \begin{bmatrix} \Psi & BE \\ 0 & T \end{bmatrix}$, $\bar{K} = [K, E]$, where $\Psi = A + BK$ is designed as Hurwitz. In order to stabilize the closed-loop system (27), we define two ellipsoidal invariant sets (39) of the extended state estimations $\hat{z}(k)$ and error $e(k)$, respectively, by

$$S_x := \{\hat{z}|\hat{z}^T(k)P_z\hat{z}(k) \leq 1\}, \tag{28}$$

and

$$S_e := \{e(k)|e^T(k)P_e e(k) \leq \bar{e}\}, \ (0 < \bar{e} \leq 1), \tag{29}$$

where P_z and P_e are both positive-definite symmetric matrices and the perturbation signal vector $D(k)$ (see Eq. (26)) is calculated by solving the following optimization problem

$$\min_{D(k)} J(k) = D^T(k)D(k),$$

$$s.t. \ \hat{z}^T(k)P_z\hat{z}(k) \leq 1. \tag{30}$$

2.4 Stability analysis
To guarantee the feasibility and stability of the control law (26), it is required to find the suitable matrices P_z and P_e assuring the invariance of S_z and S_e (see Eqs. (28) and (29)) by the following lemma.

Lemma 2. *Consider a closed-loop Hammerstein system (23) whose dynamics is determined by the output feedback control law (26) and (30) and subject to the input constraints $|u| \leq \bar{u}$, the ellipsoidal sets S_z and S_e are invariant in the sense of (28) and (29), respectively, and the control law (26) and (30) is feasible provided that Assumptions A1, A2 and the following three Assumptions A3–A5 are all fulfilled.*
A3 *The matrices Φ and Ψ are both Hurwitz;*
A4 *There exist $\tau_{1,2} > 1, 0 < \bar{e} < 1$ such that*

$$\Phi^T P_z \Phi \leq P_e, \tag{31}$$
$$\eta_1 C^T L^T E_x^T P_z E_x LC \leq P_e, \tag{32}$$
$$\tau_1 \tau_2 \Pi^T P_z \Pi + \tau_1 \eta_2 \sigma^2 \bar{K}^T B^T E_x^T P_z E_x B\bar{K},$$
$$\leq (1-\bar{e}^2)P_x, \tag{33}$$

where $\eta_1 = 1 + (\tau_1 - 1)^{-1}$, $\eta_2 = 1 + (\tau_2 - 1)^{-1}$ and

$$E_x^T = \begin{bmatrix} 1 & 0 & \cdots & \cdots & 0 \\ \vdots & \ddots & 0 & \cdots & \vdots \\ 0 & 0 & 1 & \cdots & 0 \end{bmatrix}_{N \times (N+M)}$$

is the projection matrix such that $E_x^T \hat{z}(k) = \hat{x}(k)$;

A5 There exist $\mu > 0$ and $\lambda \in (0, \bar{u})$ such that

$$|u(k)| \leq \mu |v(k)| + \lambda \tag{34}$$

(local Lipschitz condition) and

$$\begin{bmatrix} -(\bar{u} - \lambda)^2 / \mu^2 & \bar{K} \\ \bar{K}^T & -P_z \end{bmatrix} \leq 0. \tag{35}$$

Proof: We start the proof by a fact that (68), for $\forall \tau > 1$ and $\eta = 1 + (\tau - 1)^{-1}$,

$$(A_1 + A_2)^T P (A_1 + A_2)$$
$$\leq \tau A_1^T P A_1 + (1 + (\tau - 1)^{-1}) A_2^T A_2. \tag{36}$$

Thereby, one has $\forall \tau_{1,2} > 0$ and $\eta_{1,2} = 1 + (\tau_{1,2} - 1)^{-1}$, such that

$$\hat{z}^T(k + i|k) P_z \hat{z}(k + i|k) \leq \tau_1 (\Pi \hat{x}(k + i - 1|k)$$
$$+ [\delta(\cdot)(B\bar{K})^T, 0]^T x(k + \hat{i} - 1|k))^T P_z$$
$$\cdot (\Pi \hat{x}(k + i - 1|k) + [\delta(\cdot)(B\bar{K})^T, 0]^T x(k + \hat{i} - 1|k))$$
$$+ \eta_1 ([(LC)^T, 0]^T e(k + i - 1|k))^T P_z$$
$$\cdot ([(LC)^T, 0]^T e(k + i - 1|k))$$
$$\leq \tau_1 \tau_2 \hat{z}^T(k + i - 1|k) \Pi^T P_z \Pi \hat{x}(k + i - 1|k))$$
$$+ \tau_1 \eta_2 \hat{x}^T(k + i - 1|k) \sigma^2 \bar{K}^T B^T E_x^T P_z E_x \bar{K} \hat{x}(k + i - 1|k)$$
$$+ \eta_1 e^T(k + i - 1|k) C^T L^T E_x^T P_z L C e(k + i - 1|k).$$

Thereby, if Eqs. (32) and (33) hold and $\hat{z}^T(k + i - 1|k) P_z \hat{z}(k + i - 1|k) \leq 1$, then $\hat{z}^T(k + i|k) P_z \hat{z}(k + i|k) \leq 1$, i.e., S_z is an invariant set (39).

Analogously, if Eq. (31) hold and $e^T(k + i - 1|k) P_e e(k + i - 1|k) \leq \bar{e}$, then $e^T(k + i|k) P_e e(k + i|k) \leq \bar{e}$, i.e., S_e is an invariant set.

On the other hand, $|v(k)| = |\bar{K}\hat{z}(k)| = |\bar{K} P_z^{-1/2} P_z^{1/2} \bar{z}(k)| \leq \|\bar{K} P_z^{-1/2}\| \cdot \|P_z^{1/2} \bar{z}(k)\| \leq \|\bar{K} P_z^{-1/2}\|$. Taking Eq. (35) into consideration, one has

$$|v(k)| \leq (\bar{u} - \lambda_1)/\mu_1, \tag{37}$$

and substituting Eq. (37) into Eq. (34) yields $|u(k)| \leq \bar{u}$, or $u(k)$ is feasible. This completes the proof.   □

Let us explain the *dual-mode* NMPC algorithm determined by Lemma 2 as below. First, let us give the standard output feedback control law as

$$v(k) = K\hat{x}(k)$$
$$u(k) = \mathcal{N}_z^{-1}(v(k)), \tag{38}$$

and then the invariant set shrinks to

$$S_x := S_z(M = 0) = \{\hat{x}(k) | \hat{x}^T(k) P_x \hat{x}(k) \leq 1\}. \tag{39}$$

If the current $\hat{x}(k)$ moves outside of S_x, then the controller enters the *first mode*, in which the dimension of $\hat{x}(k)$ is extended from N to $N + M$ by D(k) (see Eq. (27)). Then, $\hat{x}(k)$ will be driven into S_x in no more than M steps, i.e., $\hat{x}(k + M) \in S_x$, which will also be proven later. Once $\hat{x}(k)$ enters S_x, the controller is automatically switched to the *second mode*, in which the initial control law (38) is feasible and can stabilize the system.

It has been verified by extensive experiments that assumptions A4 and A5 are not difficult to fulfil, and most of the time-consuming calculations are done off-line. First, the stable state-feedback gain K (see Eq. (26)) and observer gain L (see Eq. (24)) are pre-calculated by MATLAB. Then, compute P_e based on Eq. (29). Afterwards, pick $\mu \in (0, 1)$ and $\lambda \in (0, \bar{u})$ satisfying the local Lipschitz condition (34). Finally, pick $\tau_{1,2}$ (generally in the range (1, 1.5)), and calculate P_x off-line by MATLAB according to assumptions A4 and A5.

The aforementioned controller design is for regulator problem, or making the system state to settle down to zero. But it can be naturally extended to address the tracking problem with reference signal $r(t) = a \neq 0$. More precisely, the controller (26) is converted to $v(k) = \bar{K}\hat{z}(k) + a\rho$ with $1/\rho = \lim_{z \to 1}(\tilde{C}(zI - \Pi)^{-1}\tilde{B})$, $\tilde{C} := [C, \mathbf{0}]_{1 \times (N+M)}$ and $\tilde{B} := [B^T, \mathbf{0}]_{(N+M) \times 1}^T$. Moreover, if $I - Pi$ is nonsingular, a coordinate transformation $\hat{z}(k) - z_c \to \hat{z}(k)$ with $z_c = (I - \Pi)^{-1}\tilde{B}a\rho$ can be made to address the problem. Even if $I - \Pi$ is singular, one can still make some suitable coordinate transformation to obtain Eq. (27).

Next we will show that the dual-mode method can enlarge the closed-loop stable region. First, rewrite P_z by

$$P_z = \begin{bmatrix} (P_x)_{N \times N} & P_{xD} \\ PxD^T & (P_D)_{M \times M} \end{bmatrix},$$

and hence the maximum ellipsoid invariant set of $x(k)$ is given as

$$S_{xM} := \{\hat{x}|\hat{x}^T(P_x - P_{xD}P_D^{-1}P_{xD}^T)\hat{x}(k) \leq 1\}. \tag{40}$$

Bearing in mind that $P_x - P_{xD}P_D^{-1}P_{xD}^T = (E_x^T P_z^{-1} E_x)^{-1}$, it can be obtained that

$$\mathrm{vol}(S_{xM}) \propto \det(E_x^T P_z^{-1} E_x), \tag{41}$$

where $\mathrm{vol}(\cdot)$ and $\det(\cdot)$ denote the volume and matrix determinant. It will be verified later that the present dual-mode controller (26) can substantially enlarge the $\det(E_x^T P_z^{-1} E_x)$ with the assistance of the perturbation signal $D(k)$ and hence the closed-loop stable region S_{xM} is enlarged. Based on the above mentioned analysis of the size of the invariant set S_{xM}, we give the closed-loop stability theorem as follows.

Theorem 3. *Consider a closed-loop Hammerstein system (23) whose dynamics is determined by the output-feedback control law (26) and (30) and subject to the input constraints $|u| \leq \bar{u}$, the system is closed-loop asymptotically stable provided that assumptions A1–A5 are fulfilled.*

Proof: Based on assumptions A1–A5, one has that there exists $D(k + 1)$ such that $z(k + 1) \in S_z$ for arbitrary $x(k) \in S_x$; then by invariant property, at next sampling time $D(k + 1|k) = TD(k)$ provides a feasible choice for $D(k + 1)$ (only if $D(k) = 0$, $J(k + 1) = J(k)$, otherwise $J(k + 1) < J(k)$). Thus, the present NMPC law (26) and (30) generates a sequence of $D(k + i|k) = TD(k + i - 1|k)$ $(i = 1, \cdots, M)$ which converges to zero in M steps and ensures the input magnitudes constraints satisfaction. Certainly, it is obvious that $TD(k)$ need not have the optimal value of $D(k + 1)$ at the current time, hence the cost $J(k + 1)$ can be reduced further

still. Actually, the optimal $D^*(k+1)$ is obtained by solving Eq. (30), thus $J^*(k+1)| \leq J(k+1|k) < J(k)$ $(D(k) \neq 0)$. Therefore, as the sampling time k increases, the optimization index function $J(k)$ will decrease monotonously and $D(k)$ will converge to zero in no more than M steps. Given constraints satisfaction, the system state $\hat{x}(k)$ will enter the invariant set S_x in no more than M steps. Afterwards, the initial control law will make the closed-loop system asymptotically stable. This completes the proof.   □

2.5 Case study
2.5.1 Modeling
Consider a widely-used heat exchange process in chemical engineering as shown in Fig. 2 (17), the stream condenses in the two-pass shell and tube heat exchanger, thereby raising the temperature of process water. The relationship between the flow rate and the exit-temperature of the process water displays a Hammerstein nonlinear behavior under a fixed rate of steam flow. The condensed stream is drained through a stream trap which lets out only liquid. When the flow rate of the process water is high, the exit-temperature of stream drops below the condensation temperature at atmospheric pressure. Therefore, the steam becomes subcooled liquid, which floods the exchanger, causing the heat transfer area to decrease. Therefore, the heat transfer per unit mass of process water decreases. This is the main cause of the nonlinear dynamics.
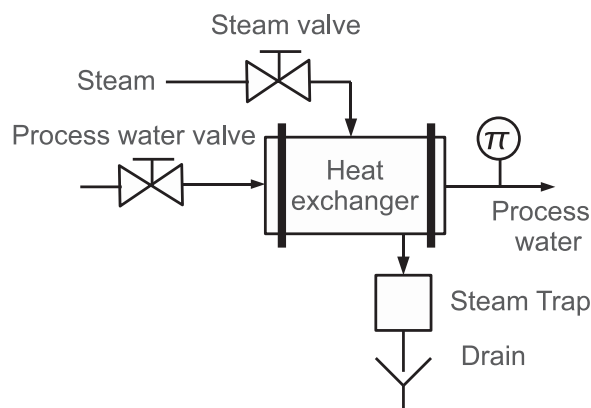

Fig. 2. Heat exchange process

The mathematical Hammerstein model describing the evolution of the exit-temperature of the process water VS the process water flow consists of the following equations (17):

$$v(t) = -31.549u(t) + 41.732u^2(t)$$
$$-24.201u^3(t) + 68.634u^4(t), \tag{42}$$

$$y(t) = \frac{0.207z^{-1} - 0.1764q^{-2}}{1 - 1.608z^{-1} + 0.6385q^{-2}}v(t) + \xi(t), \tag{43}$$

where $\xi(t)$ is a white external noise sequence with standard deviation 0.5. To simulate the fluctuations of the water flow containing variance frequencies, the input is set as periodical signal $u(t) = 0.07\cos(0.015t) + 0.455\sin(0.005t) + 0.14\sin(0.01t)$. In the numerical calculation, without loss of generality, the OFS is chosen as Laguerre series with truncation length $N = 8$, while the nonlinear bases of the nonlinear block $\mathbb{N}(\cdot)$ are selected as polynomials with $r = 9$. The sampling number $S = 2000$, and sampling period is 12s.

Note that we use odd-numbered data of the S-point to identify the coefficients $\left\{a_i^{\langle j \rangle}\right\}_{i=1}^r$ and $\left\{c_k^{\langle j \rangle}\right\}_{k=1}^N$ $(j = 1, \cdots, \eta)$, and use the even-numbered data to examine the modeling accuracy.

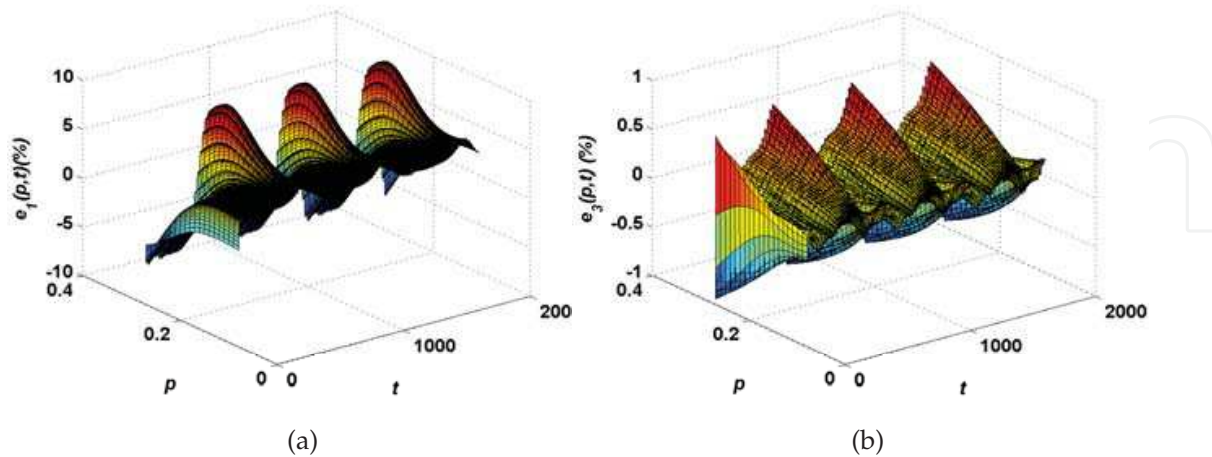(a)   (b)

Fig. 3. (Color online) (a): Modeling error of the traditional single-channel method; (b): Modeling error of the present multi-channel method (triple channels)
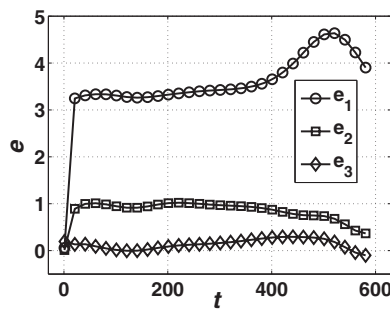

Fig. 4. Modeling error for $p = 0.1$

Denoted by $e(t)$ is the modeling error. Since the filter pole p (see Eq. (2)) plays an important role in the modeling accuracy, in Fig. 3(a) and (b), we exhibit the average modeling errors of the traditional single-channel and the present multi-channel methods along with the increase of Laguerre filter pole p. For each p, the error is obtained by averaging over 1000 independent runs. Clearly, the method proposed here has remarkably smaller modeling error than that of the traditional one. To provide more vivid contrast of these two methods, as shown in Fig. 4, we fix the Laguerre filter pole $p = 0.1$ and then calculate the average modeling errors of the single-channel ($\eta = 1$), double-channel ($\eta = 2$), and triple-channel models ($\eta = 3$) averaged over 1000 independent runs for each case. This is a standard error index to evaluate the modeling performances. The modeling error of the present method ($\eta = 3$) is reduced by more than 10 times compaired with those of the traditional one ($\eta = 1$), which vividly demonstrates the advantage of the present method.

Note that, in comparison with the traditional method, the modeling accuracy of the present approach increased by $10 - 17$ times with less than 20% increase of the computational time. So a trade off between the modeling accuracy and the computational complexity must be made. That is why here we set the optimal channel number as $\eta = 3$. The underlying reason for

the obvious slow-down of the modeling accuracy enhancement rate after $\eta = 4$ is that the 4th largest singular value σ_4 is too small compared with the largest one σ_1 (see Eq. (8)). This fact also supports the validity of the present method.

2.5.2 Control

The present dual-mode NMPC is performed in the Heat Exchanger System model (55?57) with the results shown in Figures 7,8 (Regulator Problem, $N = 2$), Figures 9?11 (Regulator Problem, $N = 3$) and Figure 12 (Tracking Problem, $N = 3$), respectively. The correspondence parameter settings are presented in Table 1.
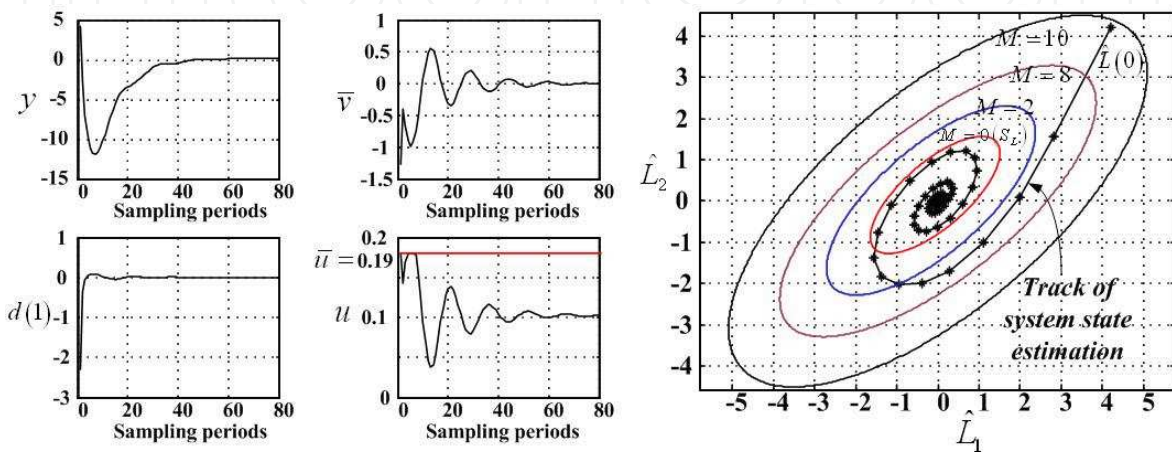

Fig. 5. (Color online) Left panel: Control performance of regulator problem ; Right panel: state trajectory L and its invariant set. Here, $N = 2$.
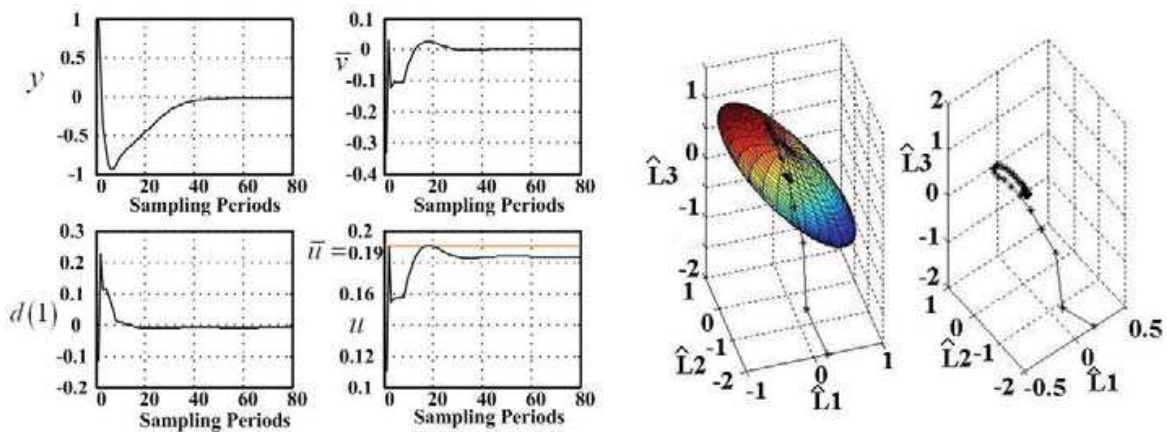

Fig. 6. (Color online) Left panel: Control performance of regulator problem ; Right panel: state trajectory L and its invariant set. Here, $N = 3$.

In these numerical examples, the initial state-feedback gain K and state observer gain Γ are optimized offline via *DLQR* and *KALMAN* functions of MATLAB6.5, respectively. The curves of $y(k)$, $u(k)$, $\bar{v}(k)$ and the first element of $D(k)$, i.e. , $d(1)$, are shown in Figure 7 (N=2) and Figure 8 (N=3), respectively. To illustrate the superiority of the proposed dual-mode NMPC, we present the curve of $\hat{L}(k)$, the invariant sets of and in Figure 8 ($N = 2$, M={2, 8, 10}) and Figure 10 and 11 ($N = 3$, $M = \{0, 5, 10\}$). One can find that $\hat{L}(0)$, is outside the feasible initial invariant set S_L (referred to (48), see the red ellipse in Figure 10 and the left subfigure of Figure
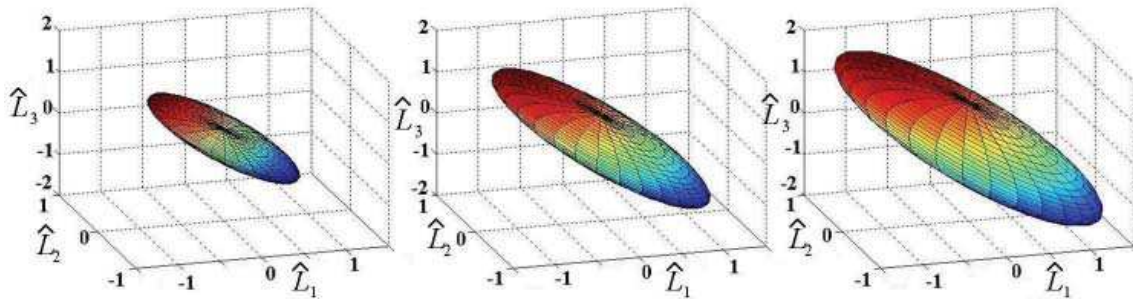
Fig. 7. (Color online) Invariant sets S_L (left) and S_{LM}, $M = 5$ (middle), $M = 3$ (right). Here, $N = 3$.
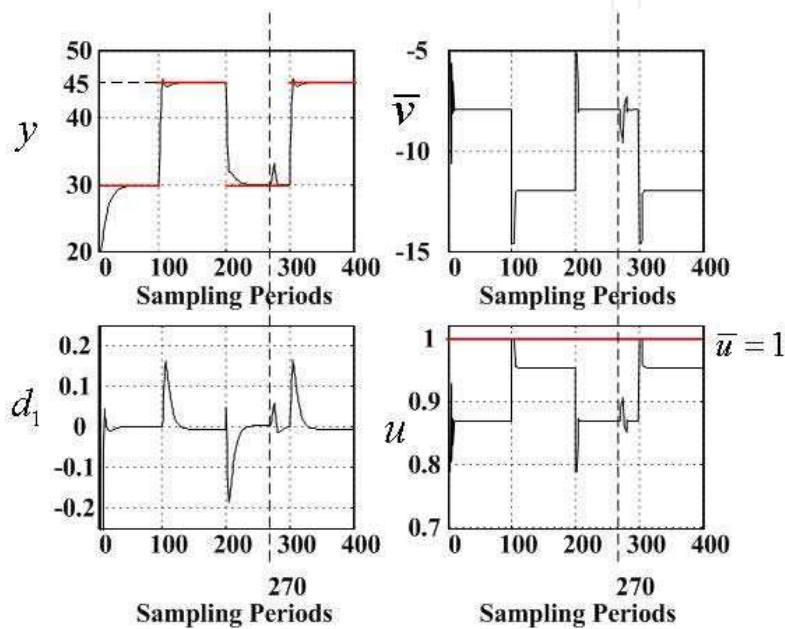

Fig. 8. (Color online) Control performances of Tracking problem.

11). Then the state extension with $M = 10$ is used to enlarge S_L to S_{LM} (referred to (52), see the black ellipse in Figure 8 and the right subfigure of Figure 11) containing $\hat{L}(0)$. After eight (Figure 8) or six steps (Figure 10), $\hat{L}(k)$ enters S_L. Afterwards, the initial control law (47) can stabilize the system and leads the state approach the origin asymptotically. Lemma 2 and Theorem 3 are thus verified. Moreover, the numerical results of Figures 8 and 11 also have verified the conclusion of the ellipsoid volume relation (54), i.e. the size of S_{LM} increases along with the enhancement of the prediction horizon M.

As to the tracking problem (see Figure 12), one should focus on the system state response to the change of the set-point. In this case, $\hat{L}(k)$ moves outside S_L, thus $D(k)$ is activated to enlarge S_L to S_{LM} and then to drive $\hat{L}(k)$ from S_L to S_{LM} in no more than steps. After 60 sampling periods, the overshooting, modulating time and steady-state error are 2.2%, 15 and 0.3% respectively. Moreover, robustness to the time-delay variations is examined at the 270-th sampling period, while the linear block of this plant is changed from (58) to

$$y(k+1) = \frac{0.207z^{-1} - 0.1764z^{-2}}{1 - 1.608z^{-1} + 0.6385z^{-2}} v(k) \tag{44}$$

dual-mode NMPC can still yield satisfactory performances, thanks to the capability of the Laguerre series in the inner model. The feasibility and superiority of the proposed control algorithm are thus demonstrated by simulations on both regulator and tracking problems.

Still worth mentioning is that some other simulations also show that the size of increases as decreases. In other words, more accurate identification and inverse solving algorithms would help further enlarge the closed-loop stable region. Fortunately, the proposed TS-SCIA can do this job quite well.

To further investigate the proposed dual-mode NMPC, a number of experiments were carried out to yield statistical results. More precisely, $\{\lambda, \mu, \tau\}$ are fixed to $\{0.70, 0.35, 1.12\}$, and N, M and σ are selected from the sets $\{2, 3, 4\}$, and $\{8, 9, \cdots, 18\}$, $\{0.001, 0.002, \cdots, 0.005\}$, respectively. The set-point is the same as Figure 12. In this set-up, 165 experiments were performed. The statistical results, such as expectations and optimal values for the settling time, overshooting, steady-state error and computational time of 400 steps are shown in Table 2. In addition, the corresponding optimal parameters are given. The statistical results further illustrate the advantages of the proposed algorithm regarding transient performance, steady-state performance and robustness to system uncertainties.

Remark 1. *The increase of the Laguerre truncation length can help enhancing the modelling and control accuracy at the cost of an increasing computational complexity. Therefore, a tradeoff must be made between accuracy and computational complexity. Note that the general parameter setting procedure is given in Remark 3.*

Parameter	Regular problem($N = 2$)	Regular problem ($N = 3$)	Tracking problem($N = 3$)
$\hat{L}(0)$	$[4.2, 4.2]^T$	$[0.02, -2, -2]^T$	$[0.02, -2, -2]^T$
K	$[0.327, -0.570]$	$[-0.328, -0.200, 0.200]$	$[-0.328, 0.200, -0.120]$
Γ	$[0.187, 0.416]^T$	$[0.217, 0.132, 0.276]^T$	$[0.217, 0.132, 0.276]^T$
$\bar{u}$	0.19	0.19	1.0
σ	0.001	0.001	10.001
μ	0.05	0.02	0.35
τ_1	1.05	1.12	1.12
τ_2	1.30	1.25	1.37
$\bar{e}$	0.5	0.5	0.5

Table 1. Parameter settings

Control indexes	STVSP (steps)	STVTD (steps)	overshooting (%)	steady-state error (%)	computational time of 400 step(s)
Optimal $\{N, M, \sigma\}$	$\{4, 7, 0.003\}$	$\{3, 12, 0.002\}$	$\{4, 8, 0.002\}$	$\{4, 10, 0.001\}$	$\{2, 8, 0.005\}$
Expectation value	16.7	12.4	±2.78	±0.41	21.062

Table 2. Statistical control performance of tracking problems, (Computation platform: 2.8G-CPU and 256M-RAML; STVSP, STVTD denote the settling times for the variations of set-point and time delay, respectively.)

2.6 Section conclusion

In this section, a novel multi-channel identification algorithm has been proposed to solve the modelling problem for constrained Hammerstein systems. Under some weak assumptions on the persistent excitation of the input, the algorithm provides consistent estimates even in the presence of colored output noise, and can eliminate any needs for prior knowledge

about the system. Moreover, it can effectively reduce the identification errors as compared to the traditional algorithms. To facilitate the controller design, the *MCIA* is converted to a two-stage identification algorithm called *TS-SCIA*, which preserve almost all the advantages of the former. In addition, to support these two algorithms, systematical analyses about their convergence and approximation capability has been provided. Based on the *TS-SCIA*, a novel dual-mode *NMPC* is developed for process control. This approach is capable of enlarging the closed-loop stable region by providing extra degrees of design freedom. Finally, modelling and control simulations have been performed on a benchmark Hammerstein system, i.e., a heat exchanger model. The statistical results have demonstrated the feasibility and superiority of the proposed identification and control algorithms for a large class of nonlinear dynamic systems often encountered in industrial processes.

3. Model Predictive Control for Wiener systems with input constraints

3.1 Introduction

The Wiener model consists of a dynamic linear filter followed by a static nonlinear subsystem. This model can approximate, with arbitrary accuracy, any nonlinear time-invariant systems (10; 23) with fading memory, thus it appears in a wide range of applications. For example, in wireless communications, the Wiener model has been shown to be appropriate for describing nonlinear power amplifiers with memory effects (15; 47). In chemistry, regulation of the pH value and identification of the distillation process have been dealt with by using the Wiener model (7; 38; 58). In biology, the Wiener model has been extensively used to describe a number of systems involving neural coding like the neural chain (47), semicircular canal primary neurons (53) and neural spike train impulses (37). Moreover, applications of the Wiener model in other complex systems such as chaotic systems have been explored (12). In fact, the control of Wiener systems has become one of the most urgently needed and yet quite difficult tasks in many relevant areas recently.

To address various control problems of Wiener systems, extensive efforts have been devoted to developing suitable MPC (model predictive control) methods. Under the MPC framework, the input is calculated by on-line minimization of the performance index based on model predictions. MPC has been practiced in industry for more than three decades and has become an industrial standard mainly due to its strong capability to deal with various constraints (23). However, to design an effective MPC, an accurate data-driven model of Wiener systems is required. A large volume of literature has been devoted to studying this issue; see (6; 24; 29; 64) for comprehensive reviews. More recently, some research interests have been focused on extending the linear subspace identification method for this typical class of nonlinear systems (23) (52) (59). Among them, Gómez's approach (23) is one of the most efficient methods since it has good prediction capabilities, and guarantees stability over a sufficiently wide range of models with different orders. In addition, this subspace method delivers a Wiener model in a format that can be directly used in a standard MPC strategy, which makes it very suitable to act as the internal model of our proposed NMPC (Nonlinear MPC) method to be further discussed below.

Nevertheless, due to its specific structure, the achievements on the control of the Wiener model are still fairly limited so far. Most of the existent control algorithms have some, if not all, of the following disadvantages:

- small asymptotically stable regions;

- limited capacity in handling input constraints;
- reliance on the detectability of the intermediate output.

For instance, Nesic (49) designs an output feedback stabilization control law for Wiener systems, but this work does not address input constraints; moreover, some rigorous conditions such as 0-state detectable are required to guarantee the global stability. Norquay *et al.* (50) and Bolemen *et al.* (7) develop NMPC strategies with ARX/polynomial and polytopic internal models, respectively, but neither considers stable region enlargement. Gómez *et al.* (23) use a subspace internal model to develop an NMPC strategy mainly accounting for unmeasurable disturbances; however, it merely inherits the stability properties of a standard linear MPC with linear constraints and quadratic cost function. Motivated by all the above-mentioned backgrounds and existing problems, the main task of this section is to develop a new efficient control algorithm for constrained Wiener systems, which can maximize the region of asymptotic stability and eliminate the reliance on the measurability of the intermediate output.

To accomplish this task, Gómez's modelling approach (23) is first used to separate the nonlinear and linear blocks of the underlying system, and then a dual-mode mechanism (14) is combined with our proposed NMPC approach to enlarge the stable region. More specifically, over a finite horizon, an optimal input profile found by solving an open-loop optimal control problem drives the nonlinear system state into the terminal invariant set (39); to that end, a linear output-feedback controller steers the state to the origin asymptotically. The main contribution of this section is the development of an algorithm that can effectively maximize the asymptotic stability region of a constrained Wiener system, by using the *dual-mode NMPC* technique, which can also eliminate the reliance on the detectability of the intermediate output (70). As a byproduct, since the nonlinear/linear blocks are separated at first and the online calculation is mainly done on the linear block, the computational complexity is remarkably reduced compared with some traditional nonlinear empirical model-based NMPCs (7; 50). Moreover, since the subspace identification method can directly yield the estimate of the nonlinear block inverse, the complex inverse-solving method is avoided in the new NMPC algorithm. Furthermore, some rigorous sufficient conditions are proposed here to guarantee the feasibility and stability of the control system.

3.2 Problem description

Consider a discrete MIMO Wiener system with a linear time-invariant (LTI) block described by

$$x(k+1) = Ax(k) + Bu(k), \tag{45}$$

$$\eta(k) = Cx(k), \tag{46}$$

and a nonlinear block by

$$y(k) = f(\eta(k)), \tag{47}$$

where $f(\cdot)$ is an invertible memoryless nonlinear function, $u(k) \in \mathbb{R}^p$, $y(k) \in \mathbb{R}^m$ are the input and output, respectively, $x(k) \in \mathbb{R}^n$ is the state vector, and $\eta(k) \in \mathbb{R}^m$ is the unmeasurable intermediate output. This Wiener system is subject to an input constraint:

$$|u_i| \leq \bar{u}_i, \ i = 1, \cdots, p. \tag{48}$$

Typically, there are two kinds of problems to consider:

- *Regulator problem*: Design an output-feedback control law such that the response of the initial conditions will die out at a desired rate;
- *Tracking problem*: Design an output-feedback control law to drive $y(t)$ to a set-point $r(k) = a$ asymptotically.

In general, for unconstrained systems with measurable $\eta(k)$, to address these two problems, one can respectively design a stable state observer,

$$\hat{x}(k+1) = A\hat{x}(k) + Bu(k) + L(\eta(k) - C\hat{x}(k)),$$

in combination with a stable state-feedback control law $u(k) = K\hat{x}(k)$ or with a stable state-feedback control law having offset (13) $u(k) = K\hat{x}(k) + a\theta$, where $1/\theta = \lim_{z\to 1}(C(zI - \Psi)^{-1}B)$ and $\Psi = A + BK$. However, for constrained Wiener systems with unmeasurable intermediate output $\eta(t)$, these basic control methods will be infeasible and the problems will become much more complex. This section develops a novel algorithm that can handle such challenging situations.

3.3 Control algorithm design

For the constrained Wiener system (45)–(48), in order to focus on the main idea of this section, i.e. dual-mode predictive mechanism, it is assumed that the system state matrices (A, B) can be estimated accurately while the identification error only appears in the output matrix estimate $\hat{C}$:

Assumption A1) the LTI matrices (A, B) can be precisely identified.

This identification can be implemented with the efficient subspace methods (23; 52; 59). In general, subspace methods give estimates of the system matrices (A, B, C). The robustness issue with estimate errors of (A, B) is beyond the scope of the current chapter, hence will not be discussed.

First, use a stable observer L to estimate $x(k)$ as follows:

$$\hat{x}(k+1) = A\hat{x}(k) + Bu(k) + L(\tilde{\eta}(k) - \hat{C}\hat{x}(k)), \tag{49}$$

where $\hat{x}(k)$ is the state estimate, and $\tilde{\eta}(k) \triangleq \hat{f}^{-1}(y(k))$ with $\hat{f}^{-1}(\cdot)$ denoting the inverse of f calculated by Gómez's subspace method (23). The state estimate error is defined as

$$e(k) \triangleq x(k) - \hat{x}(k). \tag{50}$$

Since the identified inverse $\tilde{\eta}(k)$ rather than $\eta(k)$ is used to estimate the state $x(k)$, the state estimate error $e(k)$ is caused by both the identification error of $f^{-1}(\cdot)$ and the initial condition mismatch. Therefore, the intermediate output estimate error $\hat{C}e(k)$ can be separated into two parts as follows:

$$\begin{aligned} \hat{C}e(k) &= \hat{C}x(k) - \hat{C}\hat{x}(k) \\ &= \underbrace{(\hat{C}x(k) - \tilde{\eta}(k))}_{part1} + \underbrace{(\tilde{\eta}(k) - \hat{C}\hat{x}(k))}_{part2}. \end{aligned} \tag{51}$$

Clearly, *part 1* equals $\Delta Cx(k) + \eta(k) - \tilde{\eta}(k)$ with $\Delta C = \hat{C} - C$. For a fixed nonlinear block f, *part 1* is yielded by the subspace method (23) based on state calculation, and hence the proportion of *part 1* to the whole estimate error $\hat{C}e(k)$ is solely determined by the current state

$x(k)$. It can be assumed that *part 1* of Eq. (51) satisfies the following equality:

$$\hat{C}x(k) - \tilde{\eta}(k) = \delta(x(k))\hat{C}e(k). \tag{52}$$

with $\delta(x(k)) = \text{diag}\{\delta_1(x(k)), \cdots, \delta_m(x(k))\}_{m \times m}$. For conciseness, from now on $\delta(x(k))$ and $\delta_i(x(k))$ are denoted by $\delta(\cdot)$ and $\delta_i(\cdot)$, respectively.

Next, recall the input constraint (48), and extend $\hat{x}(k)$ to $\hat{z}(k) \triangleq [\hat{x}^T(k), D^T(k)]^T$ with $D(k) \triangleq [d_1(k), \cdots, d_{H_p}(k)]^T$. Here, H_p is defined as the *prediction horizon*, and $D(k)$ represents the *auxiliary state* to be computed. Then, an extended state-feedback control law is set as

$$u(k) = K\hat{x}(k) + ED(k), \tag{53}$$

or

$$u_i(k) = K_i\hat{x}(k) + FD(k), \quad i = 1, \cdots, p, \tag{54}$$

with $K = [K_1^T, \cdots, K_p^T]^T$, $E = [F^T, \cdots, F^T]^T$ and $F = [1, 0, \cdots, 0]_{1 \times H_p}$.

Note that the novelty here lies in $D(k)$, and the reason will be demonstrated later. When the current state $x(k)$ is not in the asymptotic stability region of the constrained Wiener system (45)–(48) governed by (49) and (53), the auxiliary state $D(k)$ will be activated to drive $x(k)$ back into the asymptotic stability region in less than H_p steps, and $D(k)$ will vanish thereafter. Now, substituting (52) and (53) into (49) yields

$$\hat{z}(k+1) = \Omega\hat{z}(k) + \begin{bmatrix} L(I_m - \delta(\cdot))\hat{C} \\ \mathbf{0} \end{bmatrix} e(k), \tag{55}$$

where

$$\Omega = \begin{bmatrix} \Psi & BE \\ \mathbf{0} & M \end{bmatrix}, \quad \Psi = A + BK, \quad M = \begin{bmatrix} \mathbf{0} & I_{H_p-1} \\ 0 & \mathbf{0}^T \end{bmatrix}_{H_p \times H_p},$$

I_n is the n-dimensional identity matrix, $\mathbf{0}$ and $\mathbf{0}$ denote compatible zero matrix and zero column vector, respectively.

In order to stabilize the closed-loop system (55), define two ellipsoidal initial state invariant sets of $\hat{z}(k)$ and $e(k)$ as follows:

$$S \triangleq \{\hat{z}|\hat{z}^T P\hat{z} \leq 1\}, \tag{56}$$

$$S_e \triangleq \{e|e^T P_e e \leq \bar{e}^2, 0 \leq \bar{e} \leq 1\}, \tag{57}$$

where P and P_e are both positive definite and symmetric matrices to be computed, and $\bar{e}$ is a pre-defined constant. The auxiliary state $D(k)$ (see Eq. (53)) can be calculated by solving the following optimization problem:

$$\min_{D(k)} J(k) \triangleq D^T(k)D(k) \tag{58}$$

subject to Eq. (56). The following lemma and theorem guarantee the existence of S and S_e, and the feasibility of the control law (53).

Lemma 3. *For any constant matrices A_1, A_2 with compatible dimensions, and for any $\mu > 1$, one has*

$$(A_1 + A_2)^T P(A_1 + A_2) \leq \mu A_1^T PA_1 + \tau A_2^T PA_2,$$

where $\tau = 1 + (\mu - 1)^{-1}$ and P is a positive definite matrix.

Proof: For any $\mu > 1$, one has

$$
\begin{aligned}
(A_1 + A_2)^T P(A_1 + A_2) &= \mu A_1^T P A_1 \\
&+ (1 + (\mu - 1)^{-1}) A_2^T P A_2 - (\mu - 1)(A_1 - (\mu - 1)^{-1} A_2)^T \\
&\cdot P(A_1 - (\mu - 1)^{-1} A_2) \\
&\leq \mu A_1^T P A_1 + (1 + (\mu - 1)^{-1}) A_2^T P A_2. \qquad \blacksquare
\end{aligned}
$$

Theorem 4. *For the constrained Wiener system (45)–(48) governed by the control law (49), (53) and (58), if Assumption A1 and the following assumption A2 hold, then S and S_e defined respectively by (56) and (57) are invariant sets and the control law (53) satisfies (48).*

Assumption A2) *there exist $\sigma > 0, \mu_1 > 1, \mu_2 > 1$ and positive definite and symmetric matrices P, P_e, such that*

$$
\delta(\cdot) L^T P_e L \delta(\cdot) \leq \sigma^2 L^T P_e L \tag{59}
$$

$$
(I_m - \delta(\cdot)) L^T E_x^T P E_x L (I_m - \delta(\cdot)) \leq (1 + \sigma)^2 L^T E_x^T P E_x L, \tag{60}
$$

$$
\mu_2 \Omega^T P \Omega \leq (1 - \bar{e}^2) P, \tag{61}
$$

$$
\begin{bmatrix} -\bar{u}_i^2 & K_i \\ K_i^T & -P \end{bmatrix} \leq 0, \quad i = 1, \cdots, p, \tag{62}
$$

$$
\tau_2 (1 + \sigma)^2 \hat{C}^T L^T E_x^T P E_x L \hat{C} \leq P_e, \tag{63}
$$

$$
\mu_1 \Phi^T P_e \Phi + \tau_1 \sigma^2 \hat{C}^T L^T P_e L \hat{C} \leq P_e, \tag{64}
$$

where $\tau_1 = 1 + (\mu_1 - 1)^{-1}$, $\tau_2 = 1 + (\mu_2 - 1)^{-1}$, $\Phi = A - L\hat{C}$, $\bar{K}_i \triangleq [K_i, F]$, (Here, E_x is a matrix satisfying $\hat{x} = E_x^T \hat{z}$ and K_i and F are defined in Eq. (54)).

Proof: For any $\hat{z}(k) \in S$, it can be verified from (56) and (61) that

$$
\mu_2 \hat{z}(k) \Omega^T P \Omega \hat{z}(k) \leq (1 - \bar{e}^2) \hat{z}^T(k) P \hat{z}(k) \leq 1 - \bar{e}^2. \tag{65}
$$

Moreover, for any $e(k) \in S_e$, from (57), (60) and (63), one has

$$
\begin{aligned}
&\tau_2 e^T(k) \hat{C}^T (I_m - \delta(\cdot)) L^T E_x^T P E_x L (I_m - \delta(\cdot)) \hat{C} e(k) \\
&\leq \tau_2 (1 + \sigma)^2 e^T(k) \hat{C}^T L^T E_x^T P E_x L \hat{C} e(k) \\
&\leq e^T(k) P_e e(k) \leq \bar{e}^2.
\end{aligned} \tag{66}
$$

It follows from *Lemma 1* and (55) that

$$
\begin{aligned}
\hat{z}^T(k+1) P \hat{z}(k+1) &\leq \mu_2 \hat{z}^T(k) \Omega^T P \Omega \hat{z}(k) \\
&+ \tau_2 e(k)^T \hat{C}^T (1 - \delta(\cdot)) L^T E_x^T P E_x L (1 - \delta(\cdot)) \hat{C} e(k).
\end{aligned} \tag{67}
$$

Substituting (65) and (66) into (67) yields $\hat{z}^T(k+1) P \hat{z}^T(k+1) \leq 1$, which implies that S is an invariant set.

On the other hand, for any $e(k) \in S_e$, (49) and (50) yield that $e(k+1) = (\Phi + L\mathbf{ffi}(\cdot)\hat{C})e(k)$, thus by *Lemma 1*, for any $\mu_1 > 1$, the following inequality holds:

$$
\begin{aligned}
e^T(k+1)P_e e(k+1) &= ((\Phi + L\mathbf{ffi}(\cdot)\hat{C})e(k))^T P_e \\
&\cdot ((\Phi + L\mathbf{ffi}(\cdot)\hat{C})e(k)) \leq \mu_1 e^T(k)\Phi^T P_e \\
&\cdot \Phi e(k) + \tau_1 e^T(k)\hat{C}^T \mathbf{ffi}(\cdot)^T L^T P_e L\delta(\cdot)\hat{C}e^T(k) \\
&\leq e^T(k)(\mu_1 \Phi^T P_e \Phi + \tau_1 \hat{C}^T \mathbf{ffi}(\cdot)^T L^T P_e L\mathbf{ffi}(\cdot)\hat{C})e(k).
\end{aligned}
$$

By taking (59) and (64) into account, one has $e^T(k+1)P_e e(k+1) \leq \bar{e}^2$, i.e. S_e is an invariant set.

To satisfy the input constraint (48), rewrite the control law and get

$$
\begin{aligned}
|u_i(k)| = |\bar{K}_i\hat{z}(k)| &= |\bar{K}_i P^{-1/2} \cdot P^{1/2}\hat{z}(k)| \\
&\leq \|\bar{K}_i P^{-1/2}\| \cdot \|P^{1/2}\hat{z}(k)\|.
\end{aligned}
$$

Since $\|P^{1/2}\hat{z}(k)\| \leq 1$ from (56) and $\|\bar{K}_i P^{-1/2}\| \leq \bar{u}_i$ from (62), it immediately follows that $|u_i(k)| \leq \bar{u}_i$, $i = 1, \cdots, p$.   ■

Fig. 9. Dual-mode predictive controller structure.

Remark 2. *Both the internal matrices $L^T P_e L$ and $L^T E_x^T P E_x L$ in (59) and (60) of Assumption **A2** are positive definite and symmetric matrices. Hence these two inequalities provide a measure for the upper bound of the identification error of the nonlinear block inverse $f^{-1}(\cdot)$. Specifically, take the single-input/single-output (SISO) case as an instance for discussion. Inequalities (59) and (60) of Assumption **A2** can be simplified to*

$$
|\delta(\cdot)| \leq \sigma, \tag{68}
$$

*which is independent of P, P_e and L. Since (A, B) is estimated precisely (see Assumption **A1**), the subspace method yields sufficiently accurate local approximations of $f^{-1}(\cdot)$ and C. Consequently, as shown in (51), compared with the second part, the first part is much smaller, and it is thus a logical*

assumption that $\delta(\cdot)$ is locally bounded as given in (68) for SISO systems, or (59) and (60) for MIMO systems. As a consequence, the estimate error $\hat{C}e(k)$ is mainly caused by part2, i.e. the initial condition mismatch, and (59) and (60) can be easily satisfied in general. They will be further illustrated by a case study later. Moreover, σ is a parameter determining the stability performance of the new our approach. Note that even if the subspace can not yield sufficiently accurate $f^{-1}(\cdot)$ and C, i.e. σ is not sufficiently small, the present algorithm still works, but with shrinking invariant sets S_{xm} and S_e.

Remark 3. *It is shown by a number of simulations that Assumption A2 is not difficult to fulfill. A detailed procedure to obtain P and P_e is given here: First, the stable observer gain L (see (49)) and state-feedback gain K (see (53)) are pre-calculated by MATLAB, which is quite fast. Then, select $\mu_2 > 1$ (generally, it can be selected in the range $(1, 1.5)$), and compute P by the LMI toolbox of MATLAB according to (61), (62) and the pre-determined constant $\bar{e}$. Note that even for some unfavorable μ_2, one can still adjust the state-feedback gain K to guarantee the feasibility of P. Finally, select a suitable $\mu_1 > 1$ and calculate P_e by the LMI toolbox according to (63), (64), the pre-determined constant σ, and the pre-calculated matrix P. Furthermore, the obtained parameters L, P and P_e are substituted into (59) and (60) to verify their feasibility according to $\delta(\cdot)$, which is now available. If they can not be fulfilled, one should increase σ until it can be satisfied. Of course, for SISO systems, since (59) and (60) has been simplified to (68), this condition can be directly verified, which is independent of L, P and P_e. As a consequence, the computation time is mainly taken by the above-mentioned two LMIs composed of (61), (62) and (63), (64), respectively, whose computational complexities are both $O(N^2)$. Moreover, since L and K can be designed separately for the linear block, even for some unfavorable values of μ_2, one can still assure the feasibility of P_e by adjusting the feasible state-feedback gain L or moderately increasing σ. Certainly, suitable selections of μ_1 and μ_2 ($\mu_1 \in [1, 1.5]$ and $\mu_1 \in [1, 2]$ for example according to our numerical simulations) will accelerate the searching of P and P_e.*

Based on Theorem 4 and Eq. (58), a block diagram depicting the control structure is illustrated in Fig. 9.

Now, the main advantages of the present algorithm can be demonstrated. If $H_p = 0$, i.e. the system state dimension is not extended, then the control law (53) reduces to the standard output-feedback control law

$$u(k) = K\hat{x}(k), \tag{69}$$

and the invariant set S reduces to

$$S_x \triangleq \left\{ \hat{x} | \hat{x}^T P_x \hat{x} \leq 1 \right\}. \tag{70}$$

Here, (69) is called the initial control law, which drives $\hat{x}(k)$ to the origin asymptotically provided that the initial state estimate $\hat{x}(0)$ is inside S_x. However, S_x is the minimal case of S with $H_p = 0$, so it is very likely that $\hat{x}(0) \notin S_x$. Fortunately, it will shown later that the extension of the system state by (53) can enlarge S_x effectively so as to include $\hat{x}(0)$ in general. More precisely, if the current $\hat{x}(k)$ moves to outside S_x, then the controller enters the *First Mode*, in which the optimal input profile (49), (53), found by solving the open-loop optimal control problem (58), drives the nonlinear system state $\hat{x}$ into the terminal invariant set S_x over a finite horizon H_p, i.e. $\hat{x}(k + H_p) \in S_x$. To that end, the controller is automatically switched to the *Second Mode*, in which the local linear output-feedback control law (69) steers the state $\hat{x}(k)$ to the origin asymptotically. This approach is called the *dual-mode NMPC* method (14), and H_p is hereby called the prediction horizon.

Remark 4. *The present method focuses on the regulator problem. To address the tracking problem, as shown in the top-left part of Fig. 9, Equation (53) should be converted into a state-feedback control law with an offset, in the form of*

$$u(k) = \bar{K}\hat{z}(k) + a\theta,$$

where $1/\theta = \lim_{z \to 1}(\bar{C}(zI - \Omega)^{-1}\bar{B})$, $\bar{C} = [\hat{C}, \mathbf{0}]_{m \times (n+H_p)}$, $\bar{B} = [B^T, \mathbf{0}]^T_{(n+H_p) \times p'}$, *and the set-point* $r(k) = a$. *Furthermore, if* $(I - \Omega)$ *is nonsingular, then one can make a coordinate transformation* $\hat{z}(k) - \alpha \longrightarrow \tilde{z}(k)$, *with* $\alpha = (I - \Omega)^{-1}Ba\theta$, *so as to convert the tracking problem to the regulator problem. Even if* $(I - \Omega)$ *is singular, one can still use some suitable coordinate transformation to convert it to the regulator problem. In turn, the terminal invariant set* S_x *has hereby moves to a new place in the old state space spanned by* $\hat{x}$, *and the center of* S_x *is thus shifted from the origin to* α. *In this sense, these two control problems are equivalent, and hence the terminal set* S_x *should be recalculated once a new set-point variation occurs.*

Remark 5. *In many industrial applications, the constraints on the changing rate of the input, i.e.* $|\Delta u_i(k)| \leq \bar{v}_i$ *with* $\Delta u_i(k) \triangleq u_i(k+1) - u_i(k)$, $i = 1, \cdots, p$. *are very common. This kind of constraints can also be handled by the present method. More precisely, taking into consideration of (55), and letting* $Y \triangleq \begin{bmatrix} L(1 - \delta(\cdot))\hat{C} \\ \mathbf{0} \end{bmatrix}$, *one has*

$$\begin{aligned} |\Delta u_i(k)| &= \bar{K}_i(z(k+1) - z(k)) = |\bar{K}_i(\Omega - I)\hat{z}(k)| \\ &+ |\bar{K}_i Y e(k)| = |\bar{K}_i(\Omega - I)P^{-1/2}P^{1/2}\hat{z}(k)| \\ &+ |\bar{K}_i Y P_e^{-1/2}P_e^{1/2}e(k)|. \end{aligned}$$

Since $\|P^{1/2}\hat{z}(k)\| \leq 1$ *from (56) and* $\|P_e^{1/2}e(k)\| \leq \bar{e}$ *from (57), one has*

$$|\Delta u_i(k)| \leq \|\bar{K}_i(\Omega - I)P^{-1/2}\| + \bar{e}\|\bar{K}_i Y P_e^{-1/2}\|. \tag{71}$$

Thus, one can first compute K, L *and* P *according to Remark 3, and then substitute them into (71) to obtain a new matrix inequality of* P_e *as follows:*

$$\bar{K}_i Y P_e^{-1} Y^T \bar{K}_i^T \leq 1/\bar{e}^2 \cdot (\bar{v}_i - \|\bar{K}_i(\Omega - I)P^{-1/2}\|)^2, \tag{72}$$

or

$$\begin{bmatrix} -1/\bar{e}^2 \cdot (\bar{v}_i - \|\bar{K}(\Omega - I)P^{-1/2}\|)^2 & \bar{K}Y \\ Y^T \bar{K}^T & -P_e \end{bmatrix} \leq 0. \tag{73}$$

In this way, the constraints on the changing rate of the input, i.e. $|\Delta u_i(k)| \leq \bar{v}_i$, can be handled by introducing (73) into *Assumption A2*.

3.4 Stability analysis

Theorem 4 , provides the initial state invariant set guaranteeing the existence of $D(k)$ (see (53)), and this section focuses on maximizing the invariant set, i.e. the asymptotic stability region. Rewrite the matrix P as

$$\begin{bmatrix} (P_x)_{n \times n} & P_{xD} \\ P_{xD}^T & (P_D)_{H_p \times H_p} \end{bmatrix}$$

and define an extended invariant set of $\hat{x}$ as

$$S_{xm} \triangleq \left\{ \hat{x} | \hat{x}^T (P_x - P_{xD} P_D^{-1} P_{xD}^T) \hat{x} \leq 1 \right\}. \tag{74}$$

Moreover, denote the volume of the ellipsoidal invariant set S_{xm} by $\mathrm{vol}(S_{xm})$ and let $\det(\cdot)$ be the determinant and "$\propto$" denotes "proportional to". Accordingly, a new theorem is established to show the quantitative correlation between the size of the invariant set of $\hat{x}$ and the matrix P.

Theorem 5. *The following two conclusions hold:*
1) If $\hat{z}(k) \in S$ (see (56)), then $\hat{x}(k) \in S_{xm}$.
2) $\mathrm{vol}(S_{xm}) \propto \det(E_x^T P^{-1} E_x)$, here $\mathrm{vol}(\cdot)$ denotes the size of a set.

Proof: Since $\hat{z} \in S$, it follows from (56) that

$$\begin{aligned} &\hat{x}^T(k) P_x \hat{x}(k) \\ &\leq 1 - 2\hat{x}^T(k) P_{xD} D(k) - D^T(k) P_D D(k). \end{aligned} \tag{75}$$

In addition, it can be easily verified that

$$\begin{aligned} -P_D^{-1} P_{xD}^T \hat{x}(k) = \arg\max_{D(k)} \{ 1 - 2\hat{x}^T(k) \\ \times P_{xD} D(k) - D^T(k) P_D D(k) \}. \end{aligned} \tag{76}$$

Thus, substituting (76) into (75) yields $\hat{x}^T(k)(P_x - P_{xD} P_D^{-1} P_{xD}^T)\hat{x}(k) \leq 1$, which proves Conclusion 1). Furthermore, using $P_x - P_{xD} P_D^{-1} P_{xD}^T = (E_x^T P^{-1} E_x)^{-1}$ and (74), one can easily verify Conclusion 2). ∎
It can be seen from *Theorem 2* that the initial invariant set of $\hat{x}$ is effectively enlarged from S_x to S_{xm}. Moreover, in order to maximize S_{xm}, one may maximize $\det(E_x^T P^{-1} E_x)$ by the method detailed in (10), with calculation carried out using the *MATLAB LMI* toolbox. This maximized S_{xm} guarantees the existence of $D(k)$, or the feasibility of the present control law (53), with the largest possible probability. Consequently, based on Theorems 4 and 5, the closed-loop stability is guaranteed by the following theorem.

Theorem 6. *For the constrained Wiener system (45)–(48), if the control law (49), (53) and (58) is implemented along with stable state-feedback gain K and a stable state-observer L, and Assumptions A1–A2 hold, then the closed-loop system is asymptotically stable.*

Proof: If the current state estimate $\hat{z}(k) \in S$, then it follows from Theorem 4 that there exists $D(k+1)$ such that $\hat{z}(k+1) \in S$. Additionally, from (55) it is obvious that $\bar{D}(k+1) \triangleq MD(k)$ is always a candidate for $D(k+1)$, since it satisfies $\bar{J}(k+1) = \bar{D}^T(k+1)\bar{D}(k+1) \leq J(k)$, and one has $\bar{J}(k+1) = J(k)$ only if $D(k) = 0$. Indeed, it can be easily seen that the feasible sequence $\bar{D}(k+i)$ $(i = 1, \cdots, H_p)$ decreases to zero in H_p steps. Moreover, it can be seen that $\bar{D}(k+1)$ is not always the optimal value $D(k+1)$ (or $D^*(k+1)$) calculated by (58). Thus, one has $J^*(k+1) \leq \bar{J}(k+1) < J(k)$ for $D(k) \neq 0$, and the control law with the optimal auxiliary state $D^*(k+1)$ will converge to the initial control law in no more than H_p steps. Thereafter, controller (69) will make the system asymptotically stable. ∎

3.5 Case study

Consider a Wiener system described by (45)–(48) with

$$A = \begin{bmatrix} 2.3 & -1.2 \\ 1.0 & 0 \end{bmatrix}, \qquad B = \begin{bmatrix} 1 \\ 0 \end{bmatrix}, \quad C = [1,0],$$
$$f(\eta) = \eta^4 \sin(\eta) - \eta^5, \ \bar{u} = 1.5.$$

It can be easily verified that $f(\cdot)$ is a monotonically increasing function and is thus invertible. First, Gómez's subspace method (23) is used to identify the parameters of the linear block (A, B, C) and the inverse of the nonlinear block $f^{-1}(\eta)$. In order to demonstrate the merits of our proposed *dual-mode NMPC* algorithm, as shown in Fig. 10, we show a comparison to a traditional NMPC based on the NAARX (Nonlinear Additive AutoRegressive models with eXogeneous inputs) model (34), which is a special class of the well-known NARMAX models. This model is defined as

$$y(t) = \sum_{i=1}^{s} h_i(y(t-i)) + \sum_{j=0}^{q} g_j(u(t-j)) + \xi(t) \tag{77}$$

where $\{h_i(\cdot)\}$ and $\{g_i(\cdot)\}$ are scalar nonlinear functions, generally polynomials, and $\xi(t)$ is external white noise.

In this numerical example, $p = m = 1$, and the parameters of the present *dual-mode NMPC* are selected as follows: the initial state-feedback gain $K = [-2.3536, 1.1523]$ and the state observer gain $L = [1.0765, 0.3678]^T$ are optimized via *DLQR* and *KALMAN* functions of *MATLAB 6.5*, respectively. Prediction horizon $H_p = 6$, $\bar{e} = 0.4$, $\bar{x}(0) = [2.2, 2.2]^T$, $x(0) = [4.3, 4.8]^T$, $\mu_1 = 1.1$, $\mu_2 = 1.4$ and $\sigma = 0.1$. The estimate $\hat{C} = [1.01, 0]$. The parameters of the above traditional NMPC are: prediction horizon $H_p = 7$, control horizon $H_u = 7$, $s = 5$ and $q = 3$ (see Eq. (77)). In Fig. 10, the most interesting part is the system state response to the change of the set-point. The trajectories of $\{y, \eta\}$, u, and d_1 (see (53)) are shown in the upper, middle and lower parts of Fig. 10, respectively. In this case, after 200 sampling periods, the overshoot, settling time and steady-state error of the present *Dual-mode NMPC* are 12.2%, 15 steps, and 0.3%, respectively. The first two transient performance indexes are much smaller than the counterparts of the traditional NMPC as shown by the read curves in Fig. 10. These merits root in the dual-mode mechanism of our proposed NMPC, which can effectively enlarge the closed-loop stability region thereby improving the transient performances.

To illustrate the superiority of the proposed method more vividly, we present the curves of $x(k)$ (star-line), $\hat{x}(k)$ (circle-line) and the invariant sets S_x (see Eq. (70)), S_{xm} (see Eq. (74)) in Fig. 11. It should be noted that x and $\hat{x}$ in these two figures were implemented with coordinate transforms according to *Remark 3*. One can see that $\hat{x}(0)$ is outside the feasible initial invariant set S_x (see the solid ellipse in Fig. 11), thus $D(k)$ is activated to enlarge S_x to S_{xm} (see the dashed ellipse in Fig. 11 containing $\hat{x}(0)$), and then to drive $\hat{x}(k)$ back to S_x in no more than H_p steps. Thereafter, the initial control law (69) stabilizes the system and leads the state to approach the origin asymptotically. Remarkably, for favorable parameters like $H_p = 6$, $\bar{e} = 0.4$ and $\sigma = 0.1$, as shown in Fig. 11, the attraction region S_{xm} is much larger than the counterpart of the standard NMPC. Moreover, in Fig. 12 one can observe the dynamics of the state estimate error $e(k)$ (see (50) and the star-curve). One can observe that, when the trajectory of $e(k)$ starts from outside of S_e (see (57) and the ellipse), it will move back into S_e after no more than H_p steps and then converge to the origin asymptotically. Theorem 4 is thus verified.
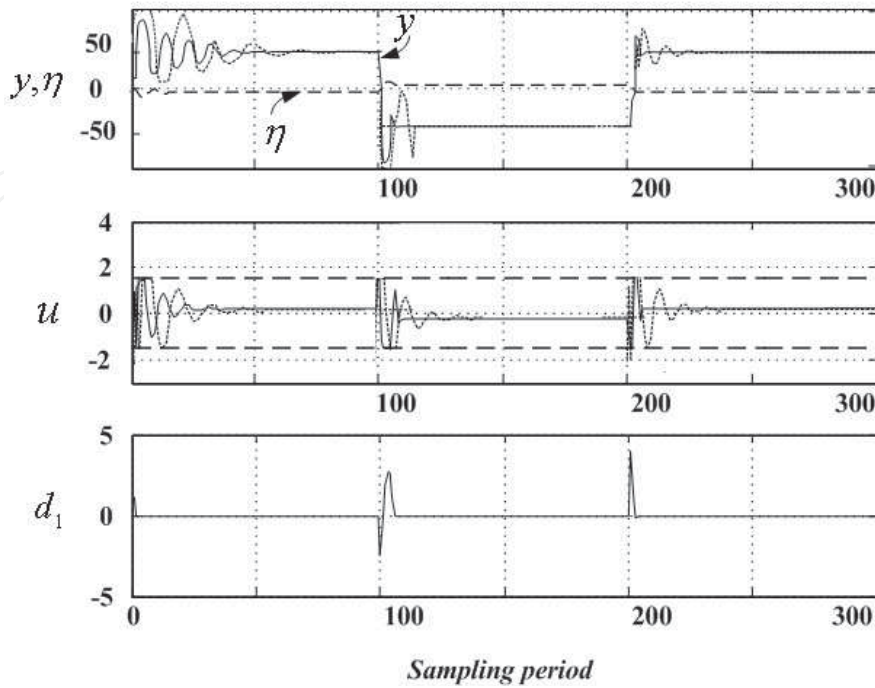
Fig. 10. Control performance comparison of the tracking problem. Solid curve: dual-mode NMPC; dotted curve: traditional NMPC; dashed curve: intermediate output (upper sub-figure) and input constraints (middle sub-figure); set-point: $\{-40, 40\}$.
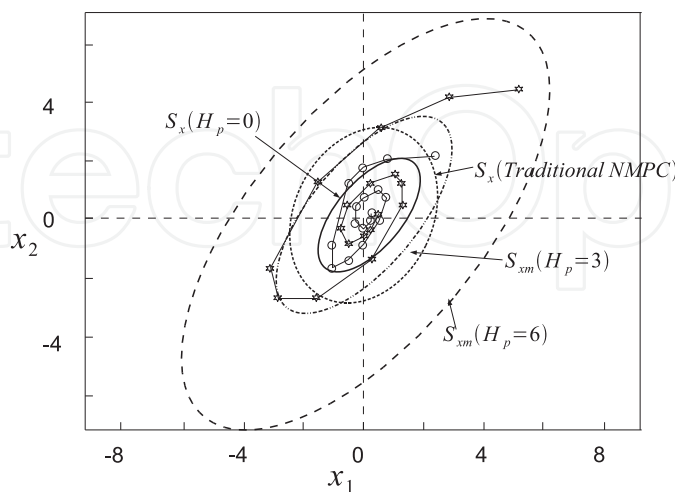
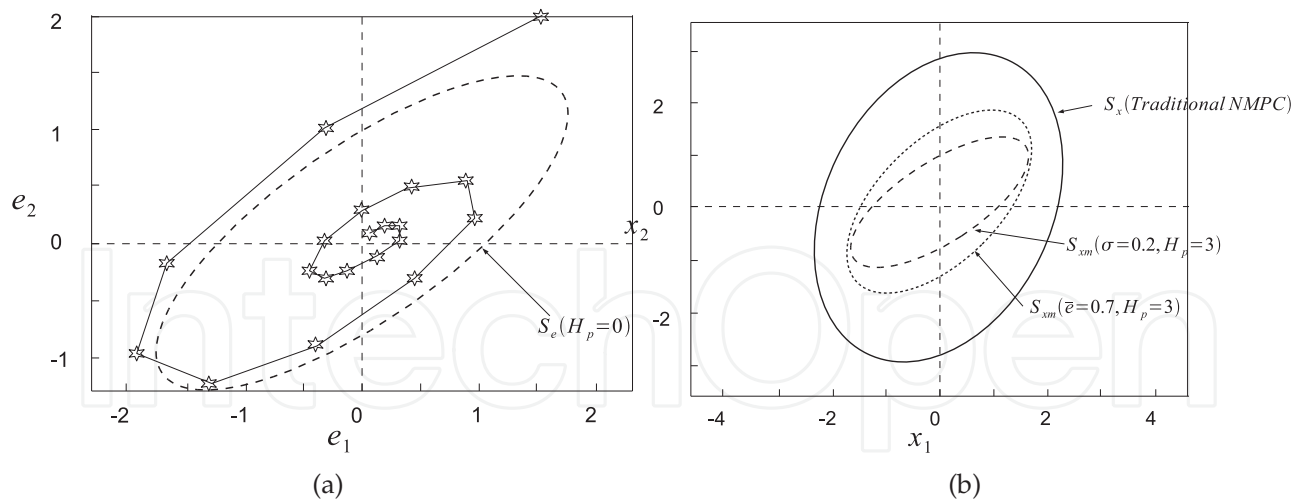

Fig. 11. Trajectory and invariant set of system states.

Fig. 12. (Color online) (a): Trajectory and invariant set of state estimate error; (b): Comparison of the invariant sets with $\sigma = 0.2$ or $\bar{e} = 0.7$.

In addition, the size comparison of S_{xm} with different $H_p \in \{0, 3, 6\}$ is presented in Fig. 11. The numerical results have verified *Theorem 5*, i.e. the size of S_{xm} increases along with the enhancement of $\det(E_x^T P^{-1} E_x)$, and the increase of H_p helps enlarge the stable region. However, this enhancement will also increase the computational complexity. Therefore, a tradeoff must be made between stability enhancement and computational load. Moreover, in order to compare the stability of the present algorithm and the traditional NMPC, their attraction regions are shown together in Fig. 11. It can be observed that the attraction region S_{xm} of the present algorithm is much larger than that of the traditional NMPC with favorable parameters.

Still worth mentioning is that some other simulations also show that the size of S_{xm} increases as σ decreases. In other words, more accurate identification algorithms would help further enlarge the asymptotic stability region. Fortunately, Gómez's method (23) is helpful in this regard. Furthermore, to verify the feasibility of (68) in *Assumption A2*, the values of $\hat{C}e(k)$ and $\hat{C}x(k) - \tilde{\eta}(k)$ are compared throughout the whole simulation process, and it is found that $|\hat{C}x(k) - \tilde{\eta}(k)| \leq \sigma|\hat{C}e(k)|$ always holds with $\sigma = 0.1$. The feasibility of Theorem 4 is thus verified.

Finally, it is remarked that the performance of the present algorithm highly depends on the effectiveness of the subspace method and the state observer L, and hence the present algorithm is not always better than NMPC. In other words, if σ or $\bar{e}$ can not be guaranteed small enough, the performance of the proposed dual-mode algorithm becomes worse than the traditional NMPC although the former is simpler and has a lower computational burden thanks to its block-oriented internal model. For instance, if $\bar{e} = 0.7$ or $\sigma = 0.2$, as shown in Fig. 12(b) (all the other parameters are the same as those in Fig. 11), the invariant set S_{xm} shrinks and becomes even smaller than that of the traditional NMPC.

3.6 Section conclusion

This section has developed an effective control method for MIMO Wiener systems with input constraints. First, the nonlinear and linear blocks of the system are separated by a subspace method. Then, a novel *dual-mode NMPC* algorithm is developed and used for the remaining process control. This approach is capable of maximizing the asymptotic stability region by

a dual-mode control mechanism, and eliminating the reliance on the measurability about the intermediate output. Finally, control simulations have demonstrated the feasibility and superiority of the proposed control algorithm for a large class of nonlinear dynamic systems. It is believed that this novel approach has promising potential in handling many complex systems often encountered in industrial control processes.

4. References

[1] Adel M. E., Makoudi M., and Radouane L., Decentralized adaptive control of linear interconnected systems based on Lauguerre series representation, *Automatica*, vol. 35, pp. 1873–1881, 1999.

[2] Bai E., An optimal two-stage identification algorithm for Hammerstein–Wiener nonlinear systems, *Automatica* vol. 34, pp. 333–338, 1998.

[3] Bai E., and Fu M., A blind approach to Hammerstein model identification, *IEEE Transactions on Acoustics, Speech, and Signal Processing* vol. 50, pp. 1610–1619, 2002.

[4] Billings S., Fakhouri Y. S., Identification of non-linear systems using correlation analysis and pseudorandom inputs, *Int. J. Systems Science* vol. 11, no. 3, pp. 261–279, 1980.

[5] Bhandari N., and Rollins D., Continuous?time Hammerstein nonlinear modelling applied to distillation, *A.I.Ch.E. Journal* vol. 50, pp. 530–533, 2004.

[6] Billings S, Fakhouri S, Identification of systems containing linear dynamic and static nonlinear elements, *Automatica* vol. 18, no. 1, pp. 15–26, 1981.

[7] Bloemen HHJ, Chou CT, van den Boom HHJ, Verdult V, Verhaegen M, Backx TC, Wiener model identification and predictive control for dual composition control of a distillation column, *Journal of Process Control* vol. 11, no. 6, pp. 601–620, 2001.

[8] Bolemen H. H. J. and Van Den Boom T. T. J., Model-based predictive control for Hammerstein systems, *Proc. 39th IEEE Conference on Decision and Control* pp. 4963–4968, 2000

[9] Bolemen H. H. J., Van Den Boom T. T. J., and Verbruggen H.B., Model-based predictive control for Hammerstein-Wiener systems, *International Journal of Control* vol. 74, pp.482–495.

[10] Boyd E., and Chua L, Fading memory and the problem of approximating nonlinear operators with Volterra series, *IEEE Transactions on Circuits and Systems* vol. 32, pp. 1150–1161, 1985.

[11] Cao M. L., Wu Z. M., Ding B. C., and Wang C. X., On the stability of two-step predictive controller based-on state observer, *Journal of Systems Engineering and Electronics*, vol. 17, pp. 132–137, 2006.

[12] Chen G, Chen Y, Ogmen H, Identifying chaotic systems via a Wiener-type cascade model, *IEEE Control System Magazine* vol. 17, no. 10, pp. 29–36, 1997.

[13] Chen C. T., *Linear System Theory and Design*, 3rd edition, Oxford University Press, 1998.

[14] Chen H., and Allgöwer F., A quasi-infinite horizon nonlinear model predictive control scheme with guaranteed stability, *Automatica* vol. 34, pp. 1205–1217, 1998.

[15] Clark C. J. , Chrisikos G., Muha M. S., Moulthrop A. A. and Silva C. P., Time-domain envelope measurement technique with application to wideband power amplifier modeling, *IEEE Transactions on Microwave Theory Tech.* vol. 46, no. 12, pp. 2531–2540, 1988.

[16] Ding B. C. and Xi Y. G., A two-step predictive control design for input saturated Hammerstein systems., *International Journal of Robust and Nonlinear Control* vol. 16, pp. 353–367, 2006.

[17] Eskinat E., and Johnson S. H., Use of Hammerstein Models in identification of Nonlinear systems, *AI.Ch.E. Journal* vol. 37, pp. 255–268, 1991.

[18] Fruzzetti K. P., Palazoglu A., and McDonald K. A., Nonlinear model predictive control using Hammerstein models, *Journal of Process Control*, vol. 7, pp. 31–41, 1997.

[19] Fu Y., and Dumont G. A., An optimum time scale for discrete Laguerre network, *IEEE Transactions on Automatic Control* vol. 38, pp. 934–938, 1993.

[20] Garcia C. E., Prett D. M., and Morari M., Model predictive control: theory and practice Đa survey, *Automatica* vol. 25, pp. 335–348, 1989.

[21] George E. F., Malcolm M. A., and Moler C. B., *Computer methods fro mathematical computations*, Prentice Hall, Inc., Englewood Cliffs, New Jersey, 1977.

[22] Golub G., and Van L. C., *Matrix Computations*, 2nd Edition, The Johns Hopkins University Press, Baltimore and London, 1989.

[23] Gómez J. C., and Baeyens E., Identification of block-oriented nonlinear systems using orthonormal basis, *Journal of Process Control* vol. 14, 685–697, 2004.

[24] Greblicki W, Nonparametric identification of Wiener systems by orthogonal series, *IEEE Transactions on Autom. Control* , vol. 39, no. 10, pp. 2077–2086, 1994.

[25] Greblicki W., Nonlinearity estimation in Hammerstein systems based on ordered observations, *IEEE Transactions on Signal Processing* vol. 44, pp. 1224–1233, 1996.

[26] Greblicki W., Stochstic approximation in nonparametric identification of Hammerstein Systems, *IEEE Transactions on Automatic Control* vol. 47, pp. 1800–1810, 2002.

[27] Greblicki W., and Pawlak M., Nonparametric identification of Hammerstein systems, *IEEE Transactions on Information Theory* vol. 35, 409–418, 1989.

[28] Haddad W. M. and Chellaboina V. S., Nonlinear control of Hammerstein systems with passive nonlinear dynamics, *IEEE Transactions on Automatic Control* vol. 46, pp. 1630–1634, 2001.

[29] Hagenblad A., *Aspects of the identification of Wiener models*, Dept. Elect. Eng., Linköping Univ., Linköping, Sweden, Tech. Rep. Licentiate, Thesis 793, Nov. 1999.

[30] Hasiewicz Z., Hammerstein system identification by the Haar multiresolution approximation, *International Journal of Adaptive Control and Signal Processing* vol. 13, pp. 691–717, 1999.

[31] Hasiewicz Z., and Mzyk G, Combined parametric-nonparametric identification of Hammerstein systems, *IEEE Transactions on Automatic Control* vol. 49, 1370–1375, 2004.

[32] Henson M. A., Nonlinear model predictive control: current status and future directions, *Computers and Chemical Engineering* vol. 23, pp. 187–202, 1998.

[33] Heuberger P. S. C., Van den Hof P. M. J., and Bosgra O. H., A generalized orthonormal basis for linear dynamical system, *IEEE Transactions on Automatic Control* vol. 40, 451–465, 1995.

[34] Henson H. A., *Nonlinear Process Control*, Prentice Hall, New Jersey, 1997.

[35] Huner I. W., and Korenberg M. J., The identification of nonlinear biological systems Wiener and Hammerstein cascade models, *Biological Cybernetics* vol. 55, pp. 135–144, 1986.

[36] Juditsky A., Hjalmarsson H., Benveniste A., Delyon B., Ljung J., Sjöberg J., and Zhang Q., Nonlinear black-box modelling in system identification: mathematical foundations, *Automatica* vol. 31, pp.1725–1750, 1995.

[37] Joeken S. and Schwegler H., Predicting spike train responses of neuron models, In *Proc. 3rd Eur. Symp. Artificial Neural Networks*, pp. 93–98, 1995.

[38] Kalafatis A., Arifin N., Wang L. and Cluett W. R., A new approach to the identification of pH processes based on the Wiener model, *Chem. Eng. Sci.* vol. 50, no. 23, pp. 3693–3701, 1995.

[39] Khalil H. K., *Nonlinear Systems* (Prentice Hall), 2002.

[40] Knohl T., Xu W. M. and H. Hubelhauen, Indirect adaptive dual control for Hammerstein systems using ANN, *Control Engineering Practice* vol. 11, pp. 277–285, 2003.

[41] Kouvaritakis B., Rossiter J. A., and Schuurmans J., Efficient robust predictive control, *IEEE Transactions on Automatic Control* vol. 45, pp. 1545–1549, 2000.

[42] Krantz S. G., *A Handbook of Real Variables: With Applications to Differential Equations and Fourier Analysis*, Birkhauser, 2004.

[43] Lakshminarayanan S. , Shah S. L. and Nandakumar K. Identification of Hammerstein models using multivariate statistical tools, *Chemical Engineering Science* vol. 50, no. 22, pp. 3599–3613, 1995.

[44] Lin Z. L. , Semi-global stabilization of discrete-time linear systems with position and rate-limited actuators. *Systems and Control Letters,* vol. 34, pp. 313–322, 1998.

[45] Liu Y, Bai E.W., Iterative identification of Hammerstein systems, *Automatica* vol. 43, no. 2, pp. 346–354, 2007.

[46] Ljung L., 1999, *System Identification: Theory for the User*, 2nd edition, Prentice-Hall, Inc. Englewood Cliffs, NJ, 1999

[47] Marmarelis VZ and Naka KI, White-noise analysis of a neuron chain: an application of the Wiener theory, *Science* vol. 175, no. 4027 pp. 1276–1278, 1972

[48] Minesh A. S., and Matthew A. F., Frequency-based controller design for a class of nonlinear systems, *International Journal of Robust and Nonlinear Control* vol. 9, pp. 825–840, 1999.

[49] Nešić D, Output feedback stabilization of a class of Wiener systems, *IEEE Transactions on Automatic Control* vol. 45, no. 9, pp. 1727–1731, 2000

[50] Norquay S. J., Palazoglu A. and Romagnoli J. A., Application of Wiener model predictive control to a pH neutralization experment, *IEEE Transactions on Control System Technology* vol. 7, no. 4, pp. 437–445, 1999.

[51] Patwardhan R., Lakshminarayanan S., and Shah S. L., 1998, Constrained nonlinear MPC using Hammerstein, *AICh.E. Journal* vol. 44, pp. 1611–1622, 1998.

[52] Raich R., Zhou G. T. and Viberg M., Subspace based approaches for Wiener system identification, *IEEE Transactions on Autom. Control* vol. 50, no.10, pp.1629–1634, 2005

[53] Segal BN, Outerbridge JS, Vestibular (semicircular canal) promary neurons in bullfrog: nonnlinearity of individual and population response to rotation, *Journal of Neurophysics* vol.47, no.4, pp. 545–562, 1982.

[54] Sjoberg J., Zhang Q., Ljung L., Benveniste A., Delyon B., Glorennec P., Hjalmarsson H., and Juditsky A., 1995, Nonlinear black-box modelling in system identification: a unified approach, *Automatica*, vol. 31, pp. 1691–1724, 1995.

[55] Stapleton J., and Bass S., Adaptive noise cancellation for a class of nonlinear dynamic reference channels, *IEEE Transactions on Circuits and Systems* vol. CAS-32, pp. 143–150, 1985

[56] Tanguy N., Morvan R., Vilbő P and Calvez L. P., Online optimization of the time scale in adaptive Laguerre-based filters. *IEEE Transactions on Signal Processing*, vol. 48, pp. 1184–1187, 2000.

[57] Tanguy N., Vilbé P., and Calvez L. C., Optimum choice of free parameter in orthonormal approximations, *IEEE Transactions on Automatic Control* vol. 40, pp. 1811–1813, 1995.

[58] Tan W. W., Lu F. and Loh A. P., An application of genetic algorithm for designing a Wiener-model controller to regulate the pH value in a pilot plant, in *Proc. 2001 Congr. Evolutionary Computation* vol. 2, pp. 1055–1061, 2001.

[59] Verhaegen M., Identification of the deterministic part of MIMO state space models given in innovations form from input-out data, *Automatica* vol. 30, no. 1, pp. 61–74, 1994.

[60] Wahlberg B. and Mäkilä P. M., On approximation of stable linear dynamic system using Laguerre and Kautz functions. *Automatica* vol. 32, pp. 693–708, 1996.

[61] Wang L., Cluett W.R., Optimal choice of time-scaling factor for linear system approximation using Laguerre models. *IEEE Transactions on Automatic Control* vol. 39, no. 7, pp. 1463–1467, 1995.

[62] Wang L. P., 2004, Discrete model predictive controller design using Laguerre functions, *Journal of Process Control* vol. 14, pp. 131–142, 2004.

[63] Westwick D. T. and Kearney R. E., Separable Least Squares Identification of Nonlinear Hammerstein Models: Application to Stretch Reflex Dynamics, *Ann. Biomed. Eng.* vol. 29, no. 8, pp. 707–718, 2001.

[64] Wigren T., Recursive prediction error identification using the nonlinear Wiener model, *Automatica* vol. 29, no. 4, pp. 1011–1025, 1993.

[65] Yuan H., Westwick D. T., Ingenito E. P., Lutchen K. R. and Suki B., Parametric and Nonparametric Nonlinear System Identification of Lung Tissue Strip Mechanics, *Ann. Biomed.Eng.* vol. 27, no. 4, pp. 548–562, 1999.

[66] Zhang H. T., Chen Z. G., Wang Y. J., Qin T., and Li M., Adaptive predictive control algorithm based on Laguerre functional model, *International Journal of Adaptive Control and Signal Processing* vol. 20, pp. 53–76, 2006.

[67] Zhang H. T., and Li H. X., A general control horizon extension method for nonlinear model predictive control, *Industrial & Engineering Chemistry Research*, vol. 46, pp. 9179–9189, 2007.

[68] Zhang H. T. , Li H. X. and Chen G. , A novel predictive control algorithm for constrained Hammerstein systems, *International Journal of Control*, vol. 81, pp. 1609–1625, 2008.

[69] Zhang H. T., Chen M. Z. Q. and Chen Z., Nonlinear Laguerre-Volterra observer-controller and its application to process control, *International Journal of Robust and Nonlinear Control*, vol.20, pp. 412–423, 2010.

[70] Zhang H. T., Chen G. and Chen M. Z. Q., A novel dual-mode predictive control strategy for constrainedWiener systems, *International Journal of Robust and Nonlinear Con- trol*,vol.20, pp. 975–986, 2010.

[71] Zhu Q. M., Warwick K., and Douce J. L., Adaptive general predictive controller for nonlinear systems, *IEE Proceedings-D* vol. 138, pp. 33–41, 1991.

Advanced Model Predictive Control

Edited by Dr. Tao ZHENG

Model Predictive Control (MPC) refers to a class of control algorithms in which a dynamic process model is used to predict and optimize process performance. From lower request of modeling accuracy and robustness to complicated process plants, MPC has been widely accepted in many practical fields. As the guide for researchers and engineers all over the world concerned with the latest developments of MPC, the purpose of "Advanced Model Predictive Control" is to show the readers the recent achievements in this area. The first part of this exciting book will help you comprehend the frontiers in theoretical research of MPC, such as Fast MPC, Nonlinear MPC, Distributed MPC, Multi-Dimensional MPC and Fuzzy-Neural MPC. In the second part, several excellent applications of MPC in modern industry are proposed and efficient commercial software for MPC is introduced. Because of its special industrial origin, we believe that MPC will remain energetic in the future.

How to reference

In order to correctly reference this scholarly work, feel free to copy and paste the following:

Hai-Tao Zhang (2011). Model Predictive Control for Block-oriented Nonlinear Systems with Input Constraints, Advanced Model Predictive Control, Dr. Tao ZHENG (Ed.), ISBN: 978-953-307-298-2, InTech, Available from: http://www.intechopen.com/books/advanced-model-predictive-control/model-predictive-control-for-block-oriented-nonlinear-systems-with-input-constraints

INTECH
open science | open minds